

Standard Model evaluation of ε_K using lattice QCD inputs for \hat{B}_K and V_{cb}

Jon A. Bailey, Yong-Chull Jang, Weonjong Lee,* and Sungwoo Park

Lattice Gauge Theory Research Center, FPRD, and CTP,

Department of Physics and Astronomy, Seoul National University, Seoul, 151-747, South Korea

(SWME Collaboration)

(Dated: December 3, 2024)

We report the Standard Model evaluation of the indirect CP violation parameter ε_K using inputs determined from lattice QCD: the kaon bag parameter \hat{B}_K , ξ_0 , $|V_{us}|$ from the $K_{\ell 3}$ and $K_{\mu 2}$ decays, and $|V_{cb}|$ from the axial current form factor for the exclusive decay $\bar{B} \rightarrow D^* \ell \bar{\nu}$ at zero-recoil. The theoretical expression for ε_K is thoroughly reviewed to give an estimate of the size of the neglected corrections, including long distance effects. The Wolfenstein parametrization ($|V_{cb}|, \lambda, \bar{\rho}, \bar{\eta}$) is adopted for CKM matrix elements which enter through the short distance contribution of the box diagrams. For the central value, we take the Unitarity Triangle apex $(\bar{\rho}, \bar{\eta})$ from the angle-only fit of the UTfit collaboration and use V_{us} as an independent input to fix λ . In order to estimate systematic error, we also use global Unitarity Triangle fit results for the parameters $(\lambda, \bar{\rho}, \bar{\eta})$ from the CKMfitter and UTfit collaborations. Taking into account all the combinations of inputs, we find that the Standard Model prediction of ε_K with exclusive V_{cb} (lattice QCD results) is lower than the experimental value by $3.6(2)\sigma$. However, with inclusive V_{cb} (results of the heavy quark expansion), there is no gap between the Standard Model prediction of ε_K and its experimental value.

PACS numbers: 11.15.Ha, 12.38.Gc, 12.38.Aw

Keywords: lattice QCD, B_K , V_{cb} , indirect CP violation, ε_K

I. INTRODUCTION

CP violation in nature was first discovered in an experiment with the neutral kaon system in 1964 [1]. There are two kinds of CP violation in the neutral kaon system: one is the indirect CP violation due to CP-asymmetric impurity in the kaon eigenstates in nature, and the other is the direct CP violation due to the CP violating nature of the weak interaction [2, 3]. CP violating observables are prime candidates in searches for physics beyond the Standard Model. Experimentally, CP violation in the neutral kaon system is known more precisely than in any other physical system. Here, we focus on the indirect CP violation in neutral kaons.

Indirect CP violation in the neutral kaon system is parametrized by ε_K

$$\varepsilon_K \equiv \frac{\mathcal{A}(K_L \rightarrow \pi\pi(I=0))}{\mathcal{A}(K_S \rightarrow \pi\pi(I=0))}, \quad (1)$$

where K_L and K_S are the neutral kaon states in nature, and $I=0$ represents the isospin of the final two-pion state. In experiment [4],

$$\begin{aligned} \varepsilon_K &= (2.228 \pm 0.011) \times 10^{-3} \times e^{i\phi_\varepsilon}, \\ \phi_\varepsilon &= 43.52 \pm 0.05^\circ. \end{aligned} \quad (2)$$

Here, the ε_K value represents an $\approx 0.2\%$ impurity of the CP even eigenstate in the K_L state, which contains 99.8% of the CP odd eigenstate.

We can also calculate ε_K directly from the Standard Model (SM). In the SM, CP violation comes solely from a

single phase in the CKM matrix elements [5, 6]. The SM allows the mixing of neutral kaons $K^0(d\bar{s})$ and $\bar{K}^0(s\bar{d})$ through loop processes, and describes contributions to the mass splitting ΔM_K and ε_K . Hence, we can test the SM through CP violation by comparing the experimental and theoretical values of ε_K .

In the SM, the master formula for ε_K that we derive in this paper is

$$\begin{aligned} \varepsilon_K &= e^{i\theta} \sqrt{2} \sin \theta \left(C_\varepsilon \hat{B}_K X_{SD} + \xi_0 + \xi_{LD} \right) \\ &+ \mathcal{O}(\omega\varepsilon') + \mathcal{O}(\xi_0 \Gamma_2 / \Gamma_1), \end{aligned} \quad (3)$$

where C_ε is a well-known coupling given in Eq. (68), and X_{SD} is the short distance contribution from the box diagrams given in Eq. (61). Here, the major contribution to ε_K comes from the \hat{B}_K term, and the minor contribution of about 7% comes from the ξ_0 term. The remaining contribution of ξ_{LD} is about 2% coming from the long distance effect on ε_K [7, 8]. A similar formula without the long distance correction ξ_{LD} and higher order terms appears in Ref. [9]. In Section II we write down explicitly the formula for the long distance and other higher order corrections.

In order to calculate ε_K directly from the SM, we use input parameters obtained from lattice QCD and experiments. In particular, \hat{B}_K and V_{cb} have dominated the statistical and systematic uncertainty in the SM evaluation of ε_K for a long time.

During the past decade, lattice QCD has made significant progress in calculating \hat{B}_K so that its error is reduced dramatically, down to the $\approx 1.3\%$ level at present. This result is available from the Flavour Lattice Averaging Group (FLAG) [10]. It is obtained by taking an average of the \hat{B}_K results from a number of lattice QCD

* E-mail: wlee@snu.ac.kr

groups [11–15]. We calculate ε_K using two different input values of \hat{B}_K : one is the FLAG result [10], and the other is the most updated result from the SWME collaboration [16].

It is also noteworthy that the lattice calculation of the amplitude $\text{Im}A_2$ related to the decay $K \rightarrow \pi\pi(I = 2)$ [17] makes it possible to determine ξ_0 more precisely.

Another important input parameter to ε_K is V_{cb} . There are two independent methods to determine V_{cb} : one is the exclusive method [18], and the other is the inclusive method [19, 20]. In the exclusive method [18], one uses lattice QCD to calculate semileptonic form factors for the decays $\bar{B} \rightarrow D^{(*)}\ell\bar{\nu}$. In the inclusive method [19, 20], one performs analysis on $B \rightarrow X_c\ell\bar{\nu}$ decay processes using the heavy quark expansion [21]. Here, we use both the exclusive and inclusive V_{cb} to determine ε_K , and we compare the results with each other and experiment.

We use the Wolfenstein parametrization for the CKM matrix [22], truncating the series at $\mathcal{O}(\lambda^7) \approx 10^{-5}$. Here, we use three different choices of Wolfenstein parameters: (1) λ , $\bar{\rho}$, and $\bar{\eta}$ from the global fit of the CKMfitter collaboration [23, 24], (2) λ , $\bar{\rho}$, and $\bar{\eta}$ from the global fit of the UTfit collaboration [25, 26], and (3) $\bar{\rho}$ and $\bar{\eta}$ from an angle-only fit (AOF) from the UTfit collaboration [27], with an independent input for λ directly from V_{us} [4]. In all the cases, we take V_{cb} instead of the Wolfenstein parameter A from the unitarity triangle (UT) analysis. We emphasize that the AOF does not use ε_K , \hat{B}_K , and V_{cb} to determine the UT apex $\bar{\rho}$ and $\bar{\eta}$. Hence, it provides a self-consistent way to test the validity of the SM with ε_K , using the lattice results for \hat{B}_K and V_{cb} with no correlation between (\hat{B}_K, V_{cb}) and $(\bar{\rho}, \bar{\eta})$.

To estimate the effect of correlations in lattice input parameters, we note that V_{cb} dominates the error in ε_K , and the FLAG \hat{B}_K [10] is dominated by the BMW collaboration result [15]. We assume that there is no correlation between the BMW \hat{B}_K and the exclusive V_{cb} from the FNAL/MILC form factor [18], because their gauge ensembles are independent. Hence, we assume that the correlation between the FLAG \hat{B}_K and the FNAL/MILC V_{cb} are negligibly small. However, when we use the SWME \hat{B}_K [16], there must be an inevitable correlation with the FNAL/MILC result for exclusive V_{cb} . In this case, we consider +50% correlation and -50% anti-correlation between the SWME \hat{B}_K and the exclusive V_{cb} to estimate the systematic error due to the correlation between them. The RBC/UKQCD collaboration calculated ξ_0 using domain-wall fermions, which is also completely independent. Hence, we assume that ξ_0 is uncorrelated with the other lattice inputs \hat{B}_K and V_{cb} .

When we determine the value of ε_K , we take into account the correlation between the SWME \hat{B}_K and the FNAL/MILC V_{cb} and assume that the other input parameters are uncorrelated. We use the Monte Carlo method to calculate the ε_K distribution from the SM. The results are cross-checked using the standard error propagation method.

In Section II, we review neutral kaon mixing and de-

rive the master formula for ε_K from the SM. Here, we give an estimate for the size of truncated small corrections. In Section III, we explain each input parameter in detail. Here, we also explain details on how we populate input distributions using the Monte Carlo method and how we determine errors on ε_K considering different input combinations and correlations among them. In Section IV, we present the results for ε_K obtained using various combinations of input parameters. In Section V, we conclude.

II. REVIEW OF ε_K

A. Effective Hamiltonian

Let us first review the theoretical formalism of neutral kaon mixing in the SM [28]. Let us consider a state that is initially (at $t = 0$) a superposition of $K^0(d\bar{s})$ and $\bar{K}^0(s\bar{d})$:

$$|\psi(0)\rangle = a(0)|K^0\rangle + b(0)|\bar{K}^0\rangle. \quad (4)$$

This state will evolve in time, and part of it will decay into final states $\{f_1, f_2, \dots\}$ as follows.

$$|\psi(t)\rangle = a(t)|K^0\rangle + b(t)|\bar{K}^0\rangle + c_1(t)|f_1\rangle + c_2(t)|f_2\rangle + \dots \quad (5)$$

If we are interested in calculating only the values of $a(t)$ and $b(t)$, but not the values of $c_i(t)$, and if the time t is much larger than the typical strong interaction scale, then we can use the simplified formalism in Ref. [29, 30]. In this formalism, the time evolution is described by a 2×2 effective Hamiltonian H_{eff} that is not Hermitian, which allows the neutral kaons to oscillate and to decay.

The neutral kaon system forms a two dimensional subspace of the Hilbert space of the total Hamiltonian $H = H_0 + H_w$. H_0 is the strong interaction Hamiltonian which defines the full Hilbert space. Decays into different strong eigenstates are mediated by the weak interaction Hamiltonian H_w , which is treated as a perturbation.

In the 2-dimensional subspace, the time evolution of the neutral kaon state vector can be described by the effective Hamiltonian H_{eff} ,

$$i\frac{d}{dt}|K(t)\rangle = H_{\text{eff}}|K(t)\rangle. \quad (6)$$

The effective Hamiltonian consists of two Hermitian operators M and Γ ,

$$H_{\text{eff}} = M - i\frac{\Gamma}{2}. \quad (7)$$

The dispersive part M defines masses of the neutral kaon states, which correspond to the kaon eigenstates in nature, and the absorptive part Γ defines decay widths of the mass eigenstates in the presence of the weak interaction H_w . The effective Hamiltonian itself, however, is not

Hermitian. It is a necessary consequence to take into account kaon decay amplitudes that have final strong eigenstates which do not belong to the neutral kaon subspace, as one can see in Eq. (5).

The decay processes can be systematically described by the perturbative corrections to the effective Hamiltonian of the subspace [31]. In the second order in H_w , or equivalently second order in the Fermi coupling constant G_F , the results are, as shown by the famous Wigner-Weisskopf formula [29, 30],

$$M_{\alpha\beta} = m_0 \delta_{\alpha\beta} + \langle \alpha | H_w | \beta \rangle - \mathcal{P} \sum_C \frac{\langle \alpha | H_w | C \rangle \langle C | H_w | \beta \rangle}{E_C - m_{K^0}}, \quad (8)$$

$$\Gamma_{\alpha\beta} = 2\pi \sum_C \langle \alpha | H_w | C \rangle \langle C | H_w | \beta \rangle \delta(E_C - m_0), \quad (9)$$

where m_{K^0} is the mass of the neutral kaons K^0 and \bar{K}^0 , \mathcal{P} denotes the principal value, $|C\rangle$ is an intermediate state with energy E_C which belongs to the full Hilbert space, and the summation over C includes integration over the continuous quantum numbers. Here, we ignore a tiny experimental mass difference between K^0 and \bar{K}^0 , since we assume CPT invariance throughout this paper. Hence, the masses of a particle and its anti-particle are the same.

The leading correction to the off-diagonal components of $M_{\alpha\beta}$ comes from the four-quark $\Delta S = 2$ operator of dimension 6. It is built from a product of two weak current-current interactions by integrating out W -bosons and heavy quarks in the box loop diagrams. This is a short distance contribution, and it is the leading effect which is responsible for the indirect CP violation in neutral kaon mixing. This short distance effect is explained in Section IIC in detail. If there exists a fundamental $\Delta S = 2$ interaction, the so-called superweak interaction H_{sw} , which is absent in the SM, it also contributes to the off-diagonal components $M_{\alpha\beta}$ [32]. Neutral kaons could decay into an intermediate state $|C\rangle$ as a result of $\Delta S = 1$ transitions. The parts which involve these intermediate states $|C\rangle$ in Eq. (8) and Eq. (9) constitute the long distance contributions.

The time independence of the effective Hamiltonian is a consequence of the Wigner-Weisskopf approximation, which takes the interaction time to infinity and turns the interaction adiabatically off [31, 33]. The well-known exponential decay law follows from this approximation. So a deviation from the conventional exponential decay gives an estimate of the accuracy of the Wigner-Weisskopf approximation. These corrections to the exponential decay, with present and foreseeable experimental precision [31, 34], are far beyond the precision that we pursue here for the value of ε_K in the SM. Hence, we neglect these corrections in this paper.

Before considering explicit calculation of the matrix elements on the right hand side of Eq. (8) and Eq. (9), we focus on their parametrization. From the Hermiticity

of M and Γ , each of them is parametrized with 4 real variables

$$M = \begin{pmatrix} M_1 & im' + \delta_{m'} \\ -im' + \delta_{m'} & M_2 \end{pmatrix}, \quad (10)$$

$$\Gamma = \begin{pmatrix} \Gamma_1 & i\gamma' + \delta_{\gamma'} \\ -i\gamma' + \delta_{\gamma'} & \Gamma_2 \end{pmatrix}. \quad (11)$$

Further simplification

$$\delta_{m'} = 0, \quad \delta_{\gamma'} = 0 \quad (12)$$

follows from CPT invariance, $(CPT)O(CPT)^{-1} = O$, where $O = M, \Gamma$, and with a specific basis made of the CP eigenstates: $\{|K_1\rangle, |K_2\rangle\}$ [32].

Assuming the strong interaction has CP symmetry, the neutral kaon subspace can be spanned by the CP even $|K_1\rangle$ and odd $|K_2\rangle$ eigenstates

$$\begin{aligned} |K_1\rangle &= \frac{1}{\sqrt{2}}(|K^0\rangle - |\bar{K}^0\rangle), \\ |K_2\rangle &= \frac{1}{\sqrt{2}}(|K^0\rangle + |\bar{K}^0\rangle). \end{aligned} \quad (13)$$

We adopt a phase convention [28]

$$CP|K^0\rangle = -|\bar{K}^0\rangle, \quad (14)$$

and for time reversal T

$$T|K^0\rangle = -|K^0\rangle, \quad T|\bar{K}^0\rangle = -|\bar{K}^0\rangle. \quad (15)$$

Here, note that the incoming state becomes an outgoing state under time reversal and vice versa. Then

$$\begin{aligned} |\bar{K}_1\rangle &= CPT|K_1\rangle = -|K_1\rangle, \\ |\bar{K}_2\rangle &= CPT|K_2\rangle = |K_2\rangle. \end{aligned} \quad (16)$$

Then we can verify the constraints in Eq. (12),

$$\begin{aligned} \langle K_1 | M | K_2 \rangle &= \langle \bar{K}_2 | (CPT)M^\dagger(CPT)^{-1} | \bar{K}_1 \rangle \\ &= -\langle K_2 | M | K_1 \rangle. \end{aligned} \quad (17)$$

The same relation also holds for Γ . Here, the Hermitian conjugate arises from the anti-unitarity of the time reversal symmetry.

B. ε_K and $\tilde{\varepsilon}$

The physical states K_S and K_L are approximately CP even and odd, respectively. In other words, the physical eigenstates of the effective Hamiltonian H_{eff} in Eq. (7) include a tiny impurity ($\approx 10^{-3}$) of the opposite CP eigenstate defined in Eq. (13). The physical eigenstates can be written with small mixing parameters $\tilde{\varepsilon}_S$ and $\tilde{\varepsilon}_L$,

$$|K_S\rangle = \frac{1}{\sqrt{1 + |\tilde{\varepsilon}_S|^2}}(|K_1\rangle + \tilde{\varepsilon}_S|K_2\rangle),$$

$$|K_L\rangle = \frac{1}{\sqrt{1 + |\tilde{\varepsilon}_L|^2}} (|K_2\rangle + \tilde{\varepsilon}_L |K_1\rangle). \quad (18)$$

Their eigenvalues are

$$\lambda_S = \bar{\lambda} - \Delta\lambda, \quad \lambda_L = \bar{\lambda} + \Delta\lambda, \quad (19)$$

where

$$\bar{\lambda} = \frac{1}{2} \left\{ (M_1 + M_2) - \frac{i}{2} (\Gamma_1 + \Gamma_2) \right\}, \quad (20)$$

$$\Delta\lambda = \frac{1}{2} \sqrt{\left(\Delta M + \frac{i}{2} \Delta\Gamma \right)^2 + 4 \left(m' - \frac{i}{2} \gamma' \right)^2}, \quad (21)$$

and

$$\Delta M = M_2 - M_1, \quad \Delta\Gamma = \Gamma_1 - \Gamma_2. \quad (22)$$

Eliminating the eigenvalues $\lambda_{S,L}$ from the system of eigenvalue equations

$$\begin{aligned} \left(M_1 - \frac{i}{2} \Gamma_1 - \lambda_S \right) + \tilde{\varepsilon}_S \left(im' + \frac{1}{2} \gamma' \right) &= 0, \\ \tilde{\varepsilon}_S \left(M_2 - \frac{i}{2} \Gamma_2 - \lambda_S \right) - \left(im' + \frac{1}{2} \gamma' \right) &= 0, \\ \left(M_2 - \frac{i}{2} \Gamma_2 - \lambda_L \right) - \tilde{\varepsilon}_L \left(im' + \frac{1}{2} \gamma' \right) &= 0, \\ \tilde{\varepsilon}_L \left(M_1 - \frac{i}{2} \Gamma_1 - \lambda_L \right) + \left(im' + \frac{1}{2} \gamma' \right) &= 0 \end{aligned} \quad (23)$$

leads to the condition

$$(\tilde{\varepsilon}_{S,L}^2 + 1) \left(im' + \frac{1}{2} \gamma' \right) - \tilde{\varepsilon}_{S,L} \left(\Delta M + \frac{i}{2} \Delta\Gamma \right) = 0 \quad (24)$$

that the mixing parameters have to satisfy. The quadratic equation in Eq. (24) has two solutions. One of them is very small ($\approx 10^{-3}$) and the other is very large ($\approx 10^{+3}$). Hence, it is obvious that the two mixing parameters are equal, since we assume that the mixing impurity is in the level of $\approx 10^{-3}$. Hence, we will use the mixing parameter $\tilde{\varepsilon}$

$$\tilde{\varepsilon} \equiv \tilde{\varepsilon}_S = \tilde{\varepsilon}_L. \quad (25)$$

Since we know that $|\tilde{\varepsilon}| \approx 10^{-3}$, we can rewrite Eq. (24) as follows,

$$\tilde{\varepsilon} = \tilde{\varepsilon}_{(0)} (1 + \tilde{\varepsilon}^2), \quad (26)$$

where

$$\tilde{\varepsilon}_{(0)} \equiv \frac{i \left(m' - \frac{i}{2} \gamma' \right)}{\Delta M + \frac{i}{2} \Delta\Gamma}. \quad (27)$$

Then, Eq. (26) can be solved iteratively near the leading order solution $\tilde{\varepsilon}_{(0)}$,

$$\tilde{\varepsilon} = \tilde{\varepsilon}_{(0)} + \tilde{\varepsilon}_{(0)}^3 + 2\tilde{\varepsilon}_{(0)}^5 + 5\tilde{\varepsilon}_{(0)}^7 + \dots \quad (28)$$

To complete the connection between $\tilde{\varepsilon}$ and ε_K , we need to consider kaon decay amplitudes [35]. Define the isospin amplitude A_I and phases ξ_I and δ_I by

$$\mathcal{A}(K^0 \rightarrow \pi\pi(I)) \equiv A_I e^{i\delta_I} = |A_I| e^{i\xi_I} e^{i\delta_I}. \quad (29)$$

Then, in our phase convention, which is one of the most popular conventions [36],

$$\mathcal{A}(\bar{K}^0 \rightarrow \pi\pi(I)) = -A_I^* e^{i\delta_I} = -|A_I| e^{-i\xi_I} e^{i\delta_I}, \quad (30)$$

and

$$\begin{aligned} \mathcal{A}(K_1 \rightarrow \pi\pi(I)) &= \sqrt{2} \text{Re} A_I e^{i\delta_I}, \\ \mathcal{A}(K_2 \rightarrow \pi\pi(I)) &= i\sqrt{2} \text{Im} A_I e^{i\delta_I}, \end{aligned} \quad (31)$$

where δ_I is the $\pi - \pi$ scattering phase shift due to the strong interaction in the final state, and the subscript I represents the isospin of the final state. Here, note that ξ_I represents the effect of the violation of Watson's theorem thanks to the violation of time reversal symmetry in the weak interaction of the SM [37], which is equivalent to the existence of direct CP violation in nature if we assume CPT invariance.

The phase δ_I is equal to the S -wave scattering phase shift of the final two-pion state by the strong interaction. Assuming isospin symmetry, this comes from Watson's theorem [35, 37]. Watson's theorem is based on time reversal symmetry implicitly. Because the final state scattering only involves H_0 , application of Watson's theorem concerns the time reversal symmetry of the strong interaction. It is equivalent to the CP symmetry, if we assume CPT invariance.

If the weak Hamiltonian H_w respected CP symmetry, which is equivalent to time reversal symmetry under CPT invariance, then Watson's theorem must hold to guarantee that A_I must be real in this case [37]. However, we know that H_w breaks CP symmetry through the existence of a single phase in the CKM matrix, and so it also violates time reversal symmetry. As a consequence, Watson's theorem is violated, and so A_I becomes complex, which generates the phase $\xi_I \neq 0$, in general. Hence, the weak phases ξ_I parametrize the direct CP violation in the weak interaction with a non-zero phase difference, $\text{Im}(A_2/A_0)$, which is independent of phase convention [28].

Now, let us focus on γ' and $\Delta\Gamma$ in Eq. (27). We will address m' and ΔM later in Section II C and Section II D. Let us divide both numerator and denominator of Eq. (27) by ΔM ; we obtain

$$\begin{aligned} \tilde{\varepsilon}_{(0)} &= e^{i\theta} \sin\theta \left(\frac{m'}{\Delta M} - i \cot\theta \frac{\gamma'}{\Delta\Gamma} \right) \\ &= e^{i\theta} \sin\theta \left(\frac{m'}{\Delta M} - i\xi_0 \cot\theta \right) + \mathcal{O}(\omega\varepsilon') \\ &\quad + \mathcal{O}(\xi_0 \Gamma_2/\Gamma_1), \end{aligned} \quad (32)$$

where

$$\tan\theta \equiv \frac{2\Delta M}{\Delta\Gamma}, \quad (33)$$

$$\begin{aligned}\varepsilon' &\equiv e^{i(\delta_2 - \delta_0)} \frac{i\omega}{\sqrt{2}} \left(\frac{\text{Im}A_2}{\text{Re}A_2} - \frac{\text{Im}A_0}{\text{Re}A_0} \right) \\ &= e^{i(\delta_2 - \delta_0)} \frac{i\omega}{\sqrt{2}} (\xi_2 - \xi_0) + \mathcal{O}(\xi_i^3),\end{aligned}\quad (34)$$

and

$$\omega \equiv \frac{\text{Re}A_2}{\text{Re}A_0}, \quad (35)$$

$$\frac{\text{Im}A_0}{\text{Re}A_0} = \tan(\xi_0) = \xi_0 + \mathcal{O}(\xi_0^3), \quad (36)$$

$$\frac{\text{Im}A_2}{\text{Re}A_2} = \tan(\xi_2) = \xi_2 + \mathcal{O}(\xi_2^3). \quad (37)$$

Here, we use the small angle approximation for the weak phases ξ_0 and ξ_2 .

When we derive Eq. (32), we apply the following approximation:

$$\frac{i\gamma'}{\Delta\Gamma} = i\xi_0 + \mathcal{O}(\omega\varepsilon') + \mathcal{O}(\xi_0\Gamma_2/\Gamma_1). \quad (38)$$

It is obtained from the fact that the neutral kaon decay amplitudes are dominated by the $I = 0$ two-pion final state. First, we can express it as follows,

$$\frac{i\gamma'}{\Delta\Gamma} = \frac{i\gamma'}{\Gamma_1} (1 + (\Gamma_2/\Gamma_1) + (\Gamma_2/\Gamma_1)^2 + \dots). \quad (39)$$

Since we know that $\Gamma_2/\Gamma_1 \approx 10^{-3}$, we can introduce the first approximation as follows,

$$\frac{i\gamma'}{\Delta\Gamma} = \frac{i\gamma'}{\Gamma_1} + \dots. \quad (40)$$

Using the Wigner-Weisskopf formula in Eq. (9), we can re-express the right-hand side as follows,

$$\frac{i\gamma'}{\Gamma_1} = \frac{\sum_C \langle K_1 | H_w | C \rangle \langle C | H_w | K_2 \rangle \delta(E_C - m_{K^0})}{\sum_C \langle K_1 | H_w | C \rangle \langle C | H_w | K_1 \rangle \delta(E_C - m_{K^0})}. \quad (41)$$

Here, it is obvious that the denominator is completely dominated by the two-pion states. In the case of the numerator, there are contributions from two-pion states, three-pion states, and so on. Here, we assume that the two-pion contribution is dominant and we may neglect the rest, which includes the (semi-)leptonic decay modes. For example, in the case of the three-pion state, the branching ratio between the two-pion decay and three-pion decay of K_S^0 is about 3.5×10^{-7} , and that for the K_L^0 is about 113 [4]. Therefore, the three-pion decay mode is suppressed by a factor of about 6.3×10^{-3} compared to the two-pion mode. Similarly, we also assume that the semi-leptonic and leptonic decay modes are so suppressed that we may neglect them in the numerator, as in Refs. [32, 38].

Therefore, as a very good approximation, we assume that the summation in C in Eq. (41) is completely dominated by the two-pion states in both the numerator and the denominator as follows.

$$A(K_1 \rightarrow C) \equiv \langle C | H_w | K_1 \rangle$$

$$\begin{aligned}&= \delta_{C,\pi\pi(0)} \langle \pi\pi(0) | H_w | K_1 \rangle + \delta_{C,\pi\pi(2)} \langle \pi\pi(2) | H_w | K_1 \rangle \\ &\quad + \dots \\ &= \delta_{C,\pi\pi(0)} \sqrt{2}(\text{Re}A_0) e^{i\delta_0} + \delta_{C,\pi\pi(2)} \sqrt{2}(\text{Re}A_2) e^{i\delta_2} \\ &\quad + \dots.\end{aligned}\quad (42)$$

Similarly,

$$\begin{aligned}A(K_2 \rightarrow C) &\equiv \langle C | H_w | K_2 \rangle \\ &= \delta_{C,\pi\pi(0)} \langle \pi\pi(0) | H_w | K_2 \rangle + \delta_{C,\pi\pi(2)} \langle \pi\pi(2) | H_w | K_2 \rangle \\ &\quad + \dots \\ &= \delta_{C,\pi\pi(0)} i\sqrt{2}(\text{Im}A_0) e^{i\delta_0} + \delta_{C,\pi\pi(2)} i\sqrt{2}(\text{Im}A_2) e^{i\delta_2} \\ &\quad + \dots.\end{aligned}\quad (43)$$

Using Eqs. (42), (43), and (41), we can obtain the following result:

$$\begin{aligned}\frac{i\gamma'}{\Gamma_1} &= \frac{2i(\text{Re}A_0)(\text{Im}A_0) + 2i(\text{Re}A_2)(\text{Im}A_2) + \dots}{2(\text{Re}A_0)^2 + 2(\text{Re}A_2)^2 + \dots} \\ &= i \left[\frac{\text{Im}A_0}{\text{Re}A_0} + \left(\frac{\text{Re}A_2}{\text{Re}A_0} \right)^2 \left\{ \frac{\text{Im}A_2}{\text{Re}A_2} - \frac{\text{Im}A_0}{\text{Re}A_0} \right\} + \dots \right] \\ &= i\xi_0 + \sqrt{2}\omega\varepsilon' e^{i(\delta_0 - \delta_2)} + \dots.\end{aligned}\quad (44)$$

Here, we know that $\xi_0 \approx 10^{-4}$ and $\sqrt{2}\omega\varepsilon' \approx 10^{-7}$. Hence we may safely neglect the $\omega\varepsilon'$ term in Eq. (44) within the precision that we pursue in this paper. This leads to the approximation in Eq. (38).

In terms of isospin amplitudes, ε_K in Eq. (1) can be written

$$\begin{aligned}\varepsilon_K &= \frac{i\text{Im}A_0 + \tilde{\varepsilon}\text{Re}A_0}{\text{Re}A_0 + i\tilde{\varepsilon}\text{Im}A_0} = \frac{\tilde{\varepsilon} + i\xi_0}{1 + i\tilde{\varepsilon}\xi_0} \\ &= (\tilde{\varepsilon} + i\xi_0)(1 - i\tilde{\varepsilon}\xi_0 + \dots) \\ &= \tilde{\varepsilon} + i\xi_0 - i\tilde{\varepsilon}^2\xi_0 + \tilde{\varepsilon}\xi_0^2 + \dots \\ &= \tilde{\varepsilon}_{(0)} + i\xi_0 + \tilde{\varepsilon}_{(0)}^3 - i\tilde{\varepsilon}_{(0)}^2\xi_0 + \dots \\ &= \tilde{\varepsilon}_{(0)} + i\xi_0 + \mathcal{O}(\tilde{\varepsilon}_{(0)}^3).\end{aligned}\quad (45)$$

Finally, using Eq. (32) and Eq. (45), we obtain

$$\begin{aligned}\varepsilon_K &= e^{i\theta} \sin\theta \left(\frac{m'}{\Delta M} + \xi_0 \right) + \mathcal{O}(\omega\varepsilon') \\ &\quad + \mathcal{O}(\xi_0\Gamma_2/\Gamma_1).\end{aligned}\quad (46)$$

Here, we keep only the first two terms from Eq. (45). The size of those corrections that we neglect in this paper is much smaller than the experimental precision of ε_K , as one can see in Eq. (2).

C. Short Distance Contribution

The matrix element m' can be calculated from the Wigner-Weisskopf formula given in Eq. (8). A short distance contribution m'_{SD} to m' is

$$2m_{K^0} \cdot im'_{\text{SD}} = \langle K_1 | \mathcal{H}_{\text{SD}}^{(6)} | K_2 \rangle$$

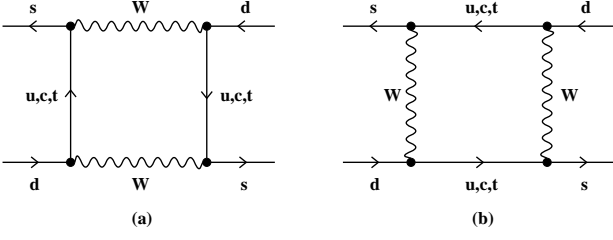


FIG. 1. Box diagrams for the $K^0 - \bar{K}^0$ mixing.

$$\begin{aligned}
&= \frac{1}{2} (\langle K^0 | \mathcal{H}_{\text{SD}}^{(6)} | \bar{K}^0 \rangle - \langle \bar{K}^0 | \mathcal{H}_{\text{SD}}^{(6)} | K^0 \rangle) \\
&= \frac{1}{2} (\langle \bar{K}^0 | \mathcal{H}_{\text{SD}}^{(6)} | K^0 \rangle^* - \langle \bar{K}^0 | \mathcal{H}_{\text{SD}}^{(6)} | K^0 \rangle) \\
&= -i \text{Im} \langle \bar{K}^0 | \mathcal{H}_{\text{SD}}^{(6)} | K^0 \rangle. \quad (47)
\end{aligned}$$

The factor $2m_{K^0}$ comes from the normalization condition for the external kaon states.

In the SM, the Hamiltonian density $\mathcal{H}_{\text{SD}}^{(6)}$ represents the leading short distance term in the $\Delta S = 2$ effective weak Hamiltonian, which is constructed from the box diagrams. For a scale below charm quark threshold $\mu < \mu_c \approx \mathcal{O}(m_c)$,

$$\begin{aligned}
\mathcal{H}_{\text{SD}}^{(6)} &= \frac{G_F^2}{16\pi^2} M_W^2 [\lambda_c^2 \eta_{cc} S_0(x_c) + \lambda_t^2 \eta_{tt} S_0(x_t) \\
&\quad + 2\lambda_c \lambda_t \eta_{ct} S_0(x_c, x_t)] b(\mu) O_{LL}^{\Delta S=2}(\mu) + h.c.. \quad (48)
\end{aligned}$$

Here, the dimension-6 local four fermion operator which comes from the well-known box diagrams in Fig. 1 is

$$O_{LL}^{\Delta S=2}(\mu) \equiv \bar{s} \gamma_\mu (1 - \gamma_5) d \bar{s} \gamma^\mu (1 - \gamma_5) d. \quad (49)$$

By integrating out the heavy degrees of freedom in the loops of the box diagrams, we obtain the Inami-Lim functions [39] as follows,

$$\begin{aligned}
S_0(x_i) &= x_i \left[\frac{1}{4} + \frac{9}{4(1-x_i)} - \frac{3}{2(1-x_i)^2} - \frac{3x_i^2 \ln x_i}{(1-x_i)^3} \right], \\
S_0(x_i, x_j) &= \left\{ \frac{x_i x_j}{x_i - x_j} \left[\frac{1}{4} + \frac{3}{2(1-x_i)} - \frac{3}{4(1-x_i)^2} \right] \ln x_i \right. \\
&\quad \left. - (i \leftrightarrow j) \right\} - \frac{3x_i x_j}{4(1-x_i)(1-x_j)}, \quad (50)
\end{aligned}$$

where, $i = c, t$, $x_i = m_i^2/M_W^2$, $m_i = m_i(m_i)$ is the scale invariant $\overline{\text{MS}}$ quark mass [40], and M_W is the W -boson pole mass. The u -quark contribution is rearranged into c and t terms by imposing a unitarity condition,

$$\begin{aligned}
\lambda_u + \lambda_c + \lambda_t &= 0, \quad (51) \\
\lambda_i &\equiv V_{is}^* V_{id},
\end{aligned}$$

and then the effective Hamiltonian $\mathcal{H}_{\text{SD}}^{(6)}$ is re-expressed with c and t terms. In Eq. (50), an approximation

$m_u^2/M_W^2 = 0$ is used. Each pair of vertices for W -boson interchange gives the products of the CKM matrix elements $\lambda_i = V_{is}^* V_{id}$.

Besides a zeroth order α_s^0 QCD effect dealt with by the Inami-Lim functions S_0 , η_{ij} with $i, j = c, t$ incorporate QCD corrections of higher order in α_s . These are obtained by resumming large logarithms with the renormalization group evolution [41]. To make it scale and renormalization scheme independent, the renormalization group running factor with 3-flavors $b(\mu)$ is factored out,

$$b(\mu) = [\alpha_s^{(3)}(\mu)]^{-2/9} K_+(\mu), \quad (52)$$

where $K_+(\mu)$ is given in Eq. (A28) of Appendix A.

It is combined with the hadronic matrix elements of the four fermion operator $O_{LL}^{\Delta S=2}(\mu)$ and used to define a renormalization group invariant quantity \hat{B}_K ,

$$\hat{B}_K \equiv B_K(\mu) b(\mu), \quad (53)$$

where

$$\begin{aligned}
B_K(\mu) &\equiv \frac{\langle \bar{K}^0 | O_{LL}^{\Delta S=2}(\mu) | K^0 \rangle}{\frac{8}{3} \langle \bar{K}^0 | \bar{s} \gamma_\mu \gamma_5 d | 0 \rangle \langle 0 | \bar{s} \gamma^\mu \gamma_5 d | K^0 \rangle} \\
&= \frac{\langle \bar{K}^0 | O_{LL}^{\Delta S=2}(\mu) | K^0 \rangle}{\frac{8}{3} F_K^2 m_{K^0}^2} \quad (54)
\end{aligned}$$

can be calculated from lattice QCD at a common scale such as $\mu = 2$ GeV. F_K is the kaon decay constant.

Inserting Eq. (48) into Eq. (47), we can identify the short distance contribution to m' as follows,

$$m'_{\text{SD}} = \frac{G_F^2}{6\pi^2} F_K^2 m_{K^0} M_W^2 \hat{B}_K X_{\text{SD}}, \quad (55)$$

where

$$\begin{aligned}
X_{\text{SD}} &= \text{Im} \lambda_t \left[\text{Re} \lambda_c \eta_{cc} S_0(x_c) - \text{Re} \lambda_t \eta_{tt} S_0(x_t) \right. \\
&\quad \left. - (\text{Re} \lambda_c - \text{Re} \lambda_t) \eta_{ct} S_0(x_c, x_t) \right]. \quad (56)
\end{aligned}$$

Here, we use another unitarity identity, $\text{Im} \lambda_t = -\text{Im} \lambda_c$. It can be shown from the unitarity condition of Eq. (51) and noting that λ_u is real in the standard parametrization.

With the Wolfenstein parametrization for the CKM matrix elements [28],

$$\text{Re} \lambda_c = -\lambda \left(1 - \frac{\lambda^2}{2} \right) \left[1 - \frac{\lambda^4}{8} - A^2 \lambda^4 (1 - \bar{\rho}) \right], \quad (57)$$

$$\text{Re} \lambda_t = -\left(1 - \frac{\lambda^2}{2} \right) A^2 \lambda^5 (1 - \bar{\rho}), \quad (58)$$

$$\text{Im} \lambda_t = \eta A^2 \lambda^5, \quad (59)$$

where

$$\bar{\rho} = \rho \left(1 - \frac{\lambda^2}{2} \right), \quad \bar{\eta} = \eta \left(1 - \frac{\lambda^2}{2} \right). \quad (60)$$

They are accurate to $\mathcal{O}(\lambda^5)$. Here, we have neglected terms of $\mathcal{O}(\lambda^7)$. Then

$$X_{\text{SD}} = \bar{\eta}\lambda^2|V_{cb}|^2 \left[|V_{cb}|^2(1-\bar{\rho})\eta_{tt}S_0(x_t)(1+r) + \left(1 - \frac{\lambda^4}{8}\right) \{\eta_{ct}S_0(x_c, x_t) - \eta_{cc}S_0(x_c)\} \right], \quad (61)$$

where $r = \{\eta_{cc}S_0(x_c) - 2\eta_{ct}S_0(x_c, x_t)\}/\{\eta_{tt}S_0(x_t)\}$. Here, note that we replace A by V_{cb} , using the relation $|V_{cb}| = A\lambda^2 + \mathcal{O}(\lambda^8)$.

D. Long Distance Contribution

In the previous section, Section II C, we explain the short distance contribution of the effective Hamiltonian $\mathcal{H}_{\text{SD}}^{(6)}$ to m' . Here, we would like to address the effect of the long distance contribution to m' .

The parts of second order in H_w in Eq. (8) and Eq. (9) correspond to the long distance contributions. The long distance contribution m'_{LD} of m' is

$$\begin{aligned} m'_{\text{LD}} &= -i\mathcal{P} \sum_C \frac{\langle K_1|H_w|C\rangle\langle C|H_w|K_2\rangle}{m_{K^0} - E_C} \\ &= -\text{Im} \left[\mathcal{P} \sum_C \frac{\langle \bar{K}^0|H_w|C\rangle\langle C|H_w|K^0\rangle}{m_{K^0} - E_C} \right] + \delta m'_{\text{LD}}, \\ \delta m'_{\text{LD}} &= \frac{1}{2}\mathcal{P} \sum_C \frac{|\langle K_0|H_w|C\rangle|^2 - |\langle \bar{K}^0|H_w|C\rangle|^2}{m_{K^0} - E_C}. \end{aligned} \quad (62)$$

Here, note that $\delta m'_{\text{LD}}$ vanishes due to CPT invariance,

$$\delta m'_{\text{LD}} = 0. \quad (63)$$

The absorptive part γ' , which comes entirely from the long distance effect, is treated in the previous section, Section II B.

The net contribution ξ_{LD} to ε_K in Eq. (3), which comes from m'_{LD} , was estimated to be the same order of magnitude as ξ_0 using chiral perturbation theory [38]. They claim that $\xi_{\text{LD}} = -0.4(3)\xi_0$ and that ξ_{LD} is at most a 4% correction to ε_K . This claim is consistent with the estimate of about 2% in Ref. [7].

Following the estimate of the long distance contribution m'_{LD} , it was claimed in Ref. [38] that this contribution should be incorporated. However, in this paper, we will neglect this long distance effect ξ_{LD} , because it is too small ($\approx 2\%$) to have any effect on our conclusion.

The theoretical expression for the mass difference ΔM defined by Eq. (22) is

$$\Delta M = 2\text{Re}\langle \bar{K}^0|H_{\text{SD}}^{(6)}|K^0\rangle + \Delta M_{\text{LD}}, \quad (64)$$

$$\Delta M_{\text{LD}} = 2\text{Re} \left[\mathcal{P} \sum_C \frac{\langle \bar{K}^0|H_w|C\rangle\langle C|H_w|K^0\rangle}{m_{K^0} - E_C} \right]. \quad (65)$$

There has been an attempt to calculate ΔM_{LD} in lattice QCD [7, 42]. Since the precision of lattice results is not as good as that of experiment, we use the experimental results for ΔM_K in this paper.

Hence, we take the experimental value of ΔM_K for ΔM in Eq. (46). This is a very good approximation,

$$\begin{aligned} \Delta M_K &= M_L - M_S = \text{Re}(\lambda_L - \lambda_S) \\ &= \text{Re} \sqrt{\left(\Delta M + \frac{i}{2}\Delta\Gamma\right)^2 (1 - 4\tilde{\varepsilon}_{(0)}^2)} \\ &= \Delta M \cdot \text{Re} \left[(1 + i \cot \theta) \sqrt{1 - 4\tilde{\varepsilon}_{(0)}^2} \right] \\ &= \Delta M \left(1 - 2\text{Re} \left[\tilde{\varepsilon}_{(0)}^2 (1 + i \cot \theta) \right] + \mathcal{O}(\tilde{\varepsilon}_{(0)}^4) \right). \end{aligned} \quad (66)$$

Here, note that $\theta \cong \pi/4$ and $\tilde{\varepsilon}_{(0)} \cong \varepsilon_K$. Hence, the difference between ΔM_K and ΔM is of $\mathcal{O}(\Delta M \tilde{\varepsilon}_{(0)}^2)$. This small correction can make a change of $\mathcal{O}(\tilde{\varepsilon}_{(0)}^3)$ in ε_K . Here, note that $\mathcal{O}(\tilde{\varepsilon}_{(0)}^3) \ll \mathcal{O}(\omega\varepsilon')$. Hence, this is so small that we neglect it.

E. Master Formula: ε_K

From Eqs. (46), (55), (61), and (62), the phenomenological expression for the indirect CP violation parameter in the SM is

$$\begin{aligned} \varepsilon_K &= e^{i\theta} \sqrt{2} \sin \theta \left(C_\varepsilon \hat{B}_K X_{\text{SD}} + \xi_0 + \xi_{\text{LD}} \right) \\ &\quad + \mathcal{O}(\omega\varepsilon') + \mathcal{O}(\xi_0\Gamma_2/\Gamma_1), \end{aligned} \quad (67)$$

where

$$C_\varepsilon = \frac{G_F^2 F_K^2 m_{K^0} M_W^2}{6\sqrt{2}\pi^2 \Delta M_K}, \quad (68)$$

$$\xi_{\text{LD}} = \frac{m'_{\text{LD}}}{\sqrt{2}\Delta M_K}. \quad (69)$$

Here, ξ_{LD} is the long distance effect of $\approx 2\%$, which we neglect in this paper. The correction terms $\mathcal{O}(\omega\varepsilon')$ and $\mathcal{O}(\xi_0\Gamma_2/\Gamma_1)$ are of order 10^{-7} , and we also neglect them in this analysis.

In Eq. (61), the parameter r is very small ($\approx 10^{-4}$) and also $\lambda^4/8 \approx 10^{-4}$. Hence, if we neglect these small terms in Eq. (61), we can obtain the same formula as in Ref. [9]. However, in this paper we keep both the r parameter and the $\lambda^4/8$ term in Eq. (61), even though they make no difference to our conclusion.

In Ref. [9], the multiplicative factor κ_ε was introduced to incorporate long distance effects ξ_{LD} , the small additive correction ξ_0 , and deviation of the angle θ from the value 45° . Since ξ_0 can be estimated from lattice QCD [17], we can treat this small contribution to ε_K explicitly.

III. DATA ANALYSIS

A. Input Parameters

The CKMfitter and UTfit groups provide the Wolfenstein parameters $\lambda, \bar{\rho}, \bar{\eta}$ and A from the global UT fit. Here, we use $\lambda, \bar{\rho}, \bar{\eta}$ from CKMfitter [23, 24] and UTfit [25, 26], and we use V_{cb} instead of A , Eq. (61). The parameters $\lambda, \bar{\rho}$, and $\bar{\eta}$ are summarized in Table I.

The parameters ε_K, \hat{B}_K , and V_{cb} are inputs to the global UT fit. Hence, the Wolfenstein parameters extracted from the global UT fit of the CKMfitter and UTfit groups contain unwanted dependence on the ε_K calculated from the master formula, Eq. (67). To self-consistently determine ε_K , we take another input set from the angle-only fit (AOF) in Ref. [27]. The AOF does not use ε_K, \hat{B}_K , and V_{cb} as inputs to determine the UT apex of $\bar{\rho}$ and $\bar{\eta}$ [27]. The AOF gives the UT apex ($\bar{\rho}, \bar{\eta}$) but not λ . We can take λ independently from the CKM matrix element V_{us} , because this is parametrized by

$$|V_{us}| = \lambda + \mathcal{O}(\lambda^7). \quad (70)$$

Here we use the average of results extracted from the K_{L3} and $K_{\mu 2}$ decays [4].

TABLE I. Wolfenstein Parameters

	CKMfitter	UTfit	AOF
λ	0.22535(65) / [4]	0.22535(65) / [4]	0.2252(9) / [4]
$\bar{\rho}$	$0.131^{+0.026}_{-0.013}$ / [4]	0.136(18) / [4]	0.130(27) / [27]
$\bar{\eta}$	$0.345^{+0.013}_{-0.014}$ / [4]	0.348(14) / [4]	0.338(16) / [27]

The input values that we use for V_{cb} are summarized in Table II. The inclusive determination considers the following inclusive decays: $B \rightarrow X_c l \nu$ and $B \rightarrow X_s \gamma$. Moments of lepton energy, hadron masses, and photon energy are measured from the relevant decay. Those moments are fit to theoretical expressions which are obtained by applying the operator product expansion (OPE) to the decay amplitude with respect to the strong coupling α_s and inverse heavy quark mass Λ/m_b . There are two schemes for the choice of b quark mass m_b in the heavy quark expansion: the kinetic scheme and the 1S scheme [4, 20]. We use the value obtained using the kinetic scheme [20], which has somewhat larger errors and also was updated more recently.

The exclusive determination considers the semi-leptonic decay of \bar{B} to D or D^* . Here, we use the most up-to-date value from the FNAL/MILC lattice calculation of the form factor $\mathcal{F}(w)$ of the semi-leptonic decay $\bar{B} \rightarrow D^* \ell \bar{\nu}$ at zero-recoil ($w = 1$) [18]. The authors of Ref. [18] used the Wilson clover action for the heavy quarks, which is tuned by the Fermilab interpretation [43] via heavy quark effective theory [44–46], with the MILC $N_f = 2 + 1$ asqtad gauge ensembles [47]. The

heavy quark symmetry and heavy quark effective theory play a key role throughout their strategies. Considering about a 1% enhancement by the electromagnetic correction $|\bar{\eta}_{EM}|$, they combined their lattice result with the HFAG average [48] of experimental values $\mathcal{F}(1)|\bar{\eta}_{EM}||V_{cb}|$ to extract $|V_{cb}|$.

TABLE II. Inclusive and exclusive $|V_{cb}|$ in units of 10^{-3} . Here, Kin. represents the kinetic scheme in the heavy quark expansion, and 1S, the 1S scheme.

Inclusive (Kin.)	Inclusive (1S)	Exclusive
42.21(78) / [20]	41.96(45)(07) / [4]	39.04(49)(53)(19) / [18]

There has been significant progress in unquenched QCD studies in lattice gauge theory since 2000. This progress makes several lattice calculations of \hat{B}_K available at $N_f = 2 + 1$ [14, 15, 49, 50]. FLAG provides various lattice results for \hat{B}_K with $N_f = 2 + 1$ and the lattice average [10]. Here, we use the $N_f = 2 + 1$ FLAG average in Ref. [10] and the SWME result as inputs, which are summarized in Table III. FLAG uses the SWME result from Ref. [14], which is not much different from the most up-to-date value [16] that we use in this analysis. The BMW calculation [15] quotes the smallest error, and it dominates the FLAG average. The SWME result [16] quotes a larger error, and its value deviates most from the FLAG average.

TABLE III. \hat{B}_K

FLAG	SWME
0.7661(99) / [10]	0.7379(47)(365) / [16]

The RBC/UKQCD collaboration provides lattice results for $\text{Im}A_2$ and ξ_0 [17]. They obtain ξ_0 (defined in Eq. (36)) using the relation

$$\text{Re}\left(\frac{\varepsilon'}{\varepsilon_K}\right) = \frac{\cos(\phi_{\varepsilon'} - \phi_\varepsilon)}{\sqrt{2}|\varepsilon_K|} \frac{\text{Re}A_2}{\text{Re}A_0} (\text{Im}A_2 - \xi_0). \quad (71)$$

In this relation, they use the lattice result for $\text{Im}A_2$ and take the experimental values for the remaining parameters to obtain ξ_0 . In particular, they use the experimental value of ε_K as an input parameter to determine ξ_0 . However, the error is dominated by the experimental error of $\text{Re}(\varepsilon'/\varepsilon_K)$, which is $\approx 14\%$. In the numerator, $\cos(\phi_{\varepsilon'} - \phi_\varepsilon)$ is approximated by 1, because the two phases are very close to each other [4],

$$\phi_\varepsilon = 43.52(5), \quad (72)$$

$$\phi_{\varepsilon'} = 42.3(15). \quad (73)$$

The final result for ξ_0 in Ref. [17] is

$$\xi_0 = -1.63(19)(20) \times 10^{-4}. \quad (74)$$

The factor η_{tt} is given at next-to-leading order (NLO) in Ref. [9]. Other factors η_{ct} and η_{cc} are given at next-to-next-to-leading order (NNLO) in Refs. [51] and [52], respectively. The NNLO values of η_{ct} and η_{cc} are larger than the NLO results in Ref. [9]:

$$\eta_{ct}^{\text{NLO}} = 0.47(4), \quad (75)$$

$$\eta_{ct}^{\text{NNLO}} = 0.496(47), \quad (76)$$

$$\eta_{cc}^{\text{NLO}} = 1.43(23), \quad (77)$$

$$\eta_{cc}^{\text{NNLO}} = 1.72(27). \quad (78)$$

Here, we quote the NNLO result for η_{cc} from SWME in Table IV, which is a major update to our previous analysis [53]. In the case of η_{cc} , the NNLO correction is as large as the NLO correction. Hence, the convergence of the perturbative series in η_{cc} is in question [52].

In Ref. [54], they claim that the error is overestimated for the NNLO value of η_{cc} given in Ref. [52]. Hence, in order to check the claim, we follow the renormalization group (RG) evolution for η_{cc} described in Ref. [52] to produce the NNLO value of η_{cc} . The results are summarized in Table IV. In this table, note that the results are consistent with one another within the systematic errors. Here, ‘‘SWME’’ represents our evaluation of η_{cc} , which is essentially identical to that of Ref. [54]. Details of our results are explained in Appendix A. In this paper, we use the SWME result for η_{cc} to obtain ε_K .

TABLE IV. Results of η_{cc} at NNLO.

collaboration	Value	Ref.
Brod and Gorbahn	1.86(76)	[52]
Buras and Gorbach	1.70(21)	[54]
SWME	1.72(27)	Appendix A

The input values for η_{ij} that we use in this paper are summarized in Table V.

TABLE V. QCD corrections

Input	Value	Ref.
η_{cc}	1.72(27)	Appendix A
η_{tt}	0.5765(65)	[9]
η_{ct}	0.496(47)	[51]

The remaining input parameters are the Fermi constant G_F , W boson mass M_W , quark masses m_q , kaon mass m_{K^0} , mass difference ΔM_K , and kaon decay constant F_K . These are summarized in Table VI.

TABLE VI. Other Input Parameters

Input	Value	Ref.
G_F	$1.1663787(6) \times 10^{-5} \text{ GeV}^{-2}$	[4]
M_W	80.385(15) GeV	[4]
$m_c(m_c)$	1.275(25) GeV	[4]
$m_t(m_t)$	163.3(2.7) GeV	[55]
θ	43.52(5) $^\circ$	[4]
m_{K^0}	497.614(24) MeV	[4]
ΔM_K	$3.484(6) \times 10^{-12} \text{ MeV}$	[4]
F_K	156.1(8) MeV	[4]

B. Error Estimate

We use the Monte Carlo method to obtain the expectation value of ε_K ,

$$\int d^d \mathbf{x} \rho(\mathbf{x}) \varepsilon_K(\mathbf{x}) = \frac{1}{N_s} \sum_{i=1}^{N_s} \varepsilon_K(x_i) + \mathcal{O}\left(\frac{1}{\sqrt{N_s}}\right), \quad (79)$$

where \mathbf{x} is a sample vector of the input parameters that we describe in the previous section. We generate $N_s = 100,000$ random sample vectors \mathbf{x} that follow the multivariate Gaussian probability distribution $\rho(\mathbf{x})$ with covariance matrix $C_{ij} = \langle \delta x_i \delta x_j \rangle$, $\delta x_i = x_i - \langle x_i \rangle$,

$$\rho(\mathbf{x}) = \mathcal{N} \exp\left(-\frac{1}{2}(\mathbf{x} - \langle \mathbf{x} \rangle)^T C^{-1}(\mathbf{x} - \langle \mathbf{x} \rangle)\right), \quad (80)$$

where \mathcal{N} is the probability density normalization factor. The dimension of a sample vector \mathbf{x} is $d = 17$, which is the total number of input parameters which appear in the master formula for ε_K , Eq. (67). We construct the covariance matrix by assuming a correlation c_{ij} between parameters x_i and x_j

$$C_{ij} = c_{ij} \sigma_i \sigma_j, \quad (-1 \leq c_{ij} \leq 1), \quad (81)$$

and using the mean $\langle x_i \rangle$ and error σ_i of the input parameter x_i given in Tables I, II, III, V, VI, and Eq. (74). When the quoted error is asymmetric, we take the larger one as a symmetric error. The actual values of the correlation matrix c_{ij} are given in Section IV.

In this numerical study, we used the GNU Scientific Library (GSL) [56]. Specifically, we used the pseudo random number generator `ranlxd2` [57] to obtain uniformly distributed random numbers. Then we convert them to the multivariate Gaussian distribution using GSL built-in functions.

To find the contribution to the total error from the error in each parameter entering the master formula for ε_K , we use the following error propagation method. For $f = |\varepsilon_K|$, the variance is

$$\sigma_f^2 = \langle [f(\mathbf{x}) - f(\langle \mathbf{x} \rangle)]^2 \rangle = \langle [\delta f(\mathbf{x})]^2 \rangle, \quad (82)$$

where

$$\delta f(\mathbf{x}) = \sum_{j=1}^N \left. \frac{\partial f(\mathbf{x})}{\partial x_j} \right|_{\langle \mathbf{x} \rangle} \delta x_j, \quad (83)$$

as a linear approximation. Then, the square of the relative error is obtained by

$$\begin{aligned} \frac{\sigma_f^2}{\langle f \rangle^2} &\approx \sum_{j,k=1}^N \left. \frac{\partial f(\mathbf{x})}{\partial x_j} \right|_{\langle \mathbf{x} \rangle} \left. \frac{\partial f(\mathbf{x})}{\partial x_k} \right|_{\langle \mathbf{x} \rangle} \frac{\langle \delta x_j \delta x_k \rangle}{\langle f \rangle^2} \\ &= \sum_{j,k=1}^N c_{jk} \cdot \left. \frac{\partial f(\mathbf{x})}{\partial x_j} \right|_{\langle \mathbf{x} \rangle} \frac{\sigma_j}{\langle f \rangle} \cdot \left. \frac{\partial f(\mathbf{x})}{\partial x_k} \right|_{\langle \mathbf{x} \rangle} \frac{\sigma_k}{\langle f \rangle}, \quad (84) \end{aligned}$$

where c_{ij} is again the correlation matrix; by definition the diagonal components are always $c_{ii} = 1$. This method of error propagation is used to cross-check our Monte Carlo result. Indeed, errors estimated by these two different methods are consistent with each other. And for the error budget in Table IX, we quote the fractional error for the parameter x_i , which is defined as

$$\left(\left. \frac{\partial f(\mathbf{x})}{\partial x_i} \right|_{\langle \mathbf{x} \rangle} \frac{\sigma_i}{\langle f \rangle} \right)^2 \Big/ \frac{\sigma_f^2}{\langle f \rangle^2}, \quad (85)$$

in percent.

IV. RESULTS

Let us define $\varepsilon_K^{\text{SM}}$ as the theoretical evaluation of $|\varepsilon_K|$ obtained using the master formula, Eq. (67). We define $\varepsilon_K^{\text{Exp}}$ as the experimental value of $|\varepsilon_K|$, given in Eq. (2). Let us define $\Delta\varepsilon_K$ as the difference between $\varepsilon_K^{\text{Exp}}$ and $\varepsilon_K^{\text{SM}}$:

$$\Delta\varepsilon_K \equiv \varepsilon_K^{\text{Exp}} - \varepsilon_K^{\text{SM}}. \quad (86)$$

Here, we assume that the theoretical phase θ in Eq. (67) is equal to the experimental phase ϕ_ε in Eq. (2) [4].

In Table VII, we present results for $\varepsilon_K^{\text{SM}}$ obtained using the FLAG average for \hat{B}_K [10] and V_{cb} from both inclusive [20] and exclusive channels [18]. The corresponding probability distributions for $\varepsilon_K^{\text{SM}}$ and $\varepsilon_K^{\text{Exp}}$ are presented in Fig. 2. The corresponding results for $\Delta\varepsilon_K$ are presented in Table VIII.

From Table VIII, we find that $\varepsilon_K^{\text{SM}}$ with inclusive V_{cb} is consistent with $\varepsilon_K^{\text{Exp}}$ within 1σ . In other words, $\Delta\varepsilon_K$ is consistent with zero with inclusive V_{cb} regardless of the input methods.

However, from Tables VII and VIII, $\varepsilon_K^{\text{SM}}$ with exclusive V_{cb} is only 71% of $\varepsilon_K^{\text{Exp}}$. For this case, with the most reliable input method (AOF), $\Delta\varepsilon_K$ is 3.6σ . Since the largest contribution in our estimate of $\varepsilon_K^{\text{SM}}$ that we neglect is $\xi_{\text{LD}} \approx 2\%$, the neglected contributions cannot explain the gap $\Delta\varepsilon_K$ of 29% with exclusive V_{cb} . Hence, our final results for $\Delta\varepsilon_K$ are

$$\Delta\varepsilon_K = 3.6(2)\sigma \quad (\text{exclusive } V_{cb}), \quad (87)$$

TABLE VII. $\varepsilon_K^{\text{SM}}$ in units of 10^{-3} . Here, we use the FLAG average for \hat{B}_K in Table III. The input methods of CKMfitter, UTfit, and AOF represent different inputs for the Wolfenstein parameters, which are explained in detail in Section III A.

Input Method	Inclusive V_{cb}	Exclusive V_{cb}
CKMfitter	2.17(23)	1.62(18)
UTfit	2.18(22)	1.63(18)
AOF	2.13(23)	1.58(18)

TABLE VIII. $\Delta\varepsilon_K$. Here, we use $\varepsilon_K^{\text{SM}}$ from Table VII. We obtain σ by combining the errors of $\varepsilon_K^{\text{SM}}$ and $\varepsilon_K^{\text{Exp}}$ in quadrature.

Input Method	Inclusive V_{cb}	Exclusive V_{cb}
CKMfitter	0.24 σ	3.4 σ
UTfit	0.20 σ	3.4 σ
AOF	0.44 σ	3.6 σ

$$\Delta\varepsilon_K = 0.44(24)\sigma \quad (\text{inclusive } V_{cb}), \quad (88)$$

where we take the AOF result as the central value and the systematic error is obtained by taking the maximum difference among various input methods in Table VIII.

In the case of the FLAG \hat{B}_K , the BMW result for \hat{B}_K [15] dominates the FLAG result, and the gauge ensembles used for the BMW calculation are independent of those used for the determination of exclusive V_{cb} [18] by the FNAL/MILC collaboration. Hence, we assume that we may neglect the correlation between the FLAG \hat{B}_K and the exclusive V_{cb} . However, the SWME \hat{B}_K calculation in Ref. [16] shares the same MILC gauge ensembles with the exclusive V_{cb} determination in Ref. [18]. Hence, in this case, we cannot neglect the correlation between the SWME \hat{B}_K and the exclusive V_{cb} . We introduce +50% correlation and -50% anti-correlation between the SWME \hat{B}_K and the exclusive V_{cb} , and take the maximum deviation from the uncorrelated case as the systematic error due to the unknown correlation between them. The details of this analysis are explained in Appendix B. However, this analysis shows that the size of the ambiguity due to the correlation between the SWME \hat{B}_K and the exclusive V_{cb} is much larger than the systematic error in $\Delta\varepsilon_K$ with the FLAG \hat{B}_K . Hence, we use the results of the SWME \hat{B}_K only to cross-check those with the FLAG \hat{B}_K . This analysis of the correlation is another update from the previous paper [53].

It is interesting to understand the historical evolution of $\Delta\varepsilon_K/\sigma$ along with the theoretical progress in lattice QCD and perturbative QCD. In Fig. 3, we present $\Delta\varepsilon_K/\sigma$ as a function of time. In 2012, the RBC/UKQCD collaboration reported ξ_0 in Ref. [17]. In addition to this, using the LLV average for \hat{B}_K [58], the SWME collaboration reported $\Delta\varepsilon_K = 2.7(2)\sigma$ in Ref. [59] in 2012. In 2014, FNAL/MILC reported an updated V_{cb} in the exclu-

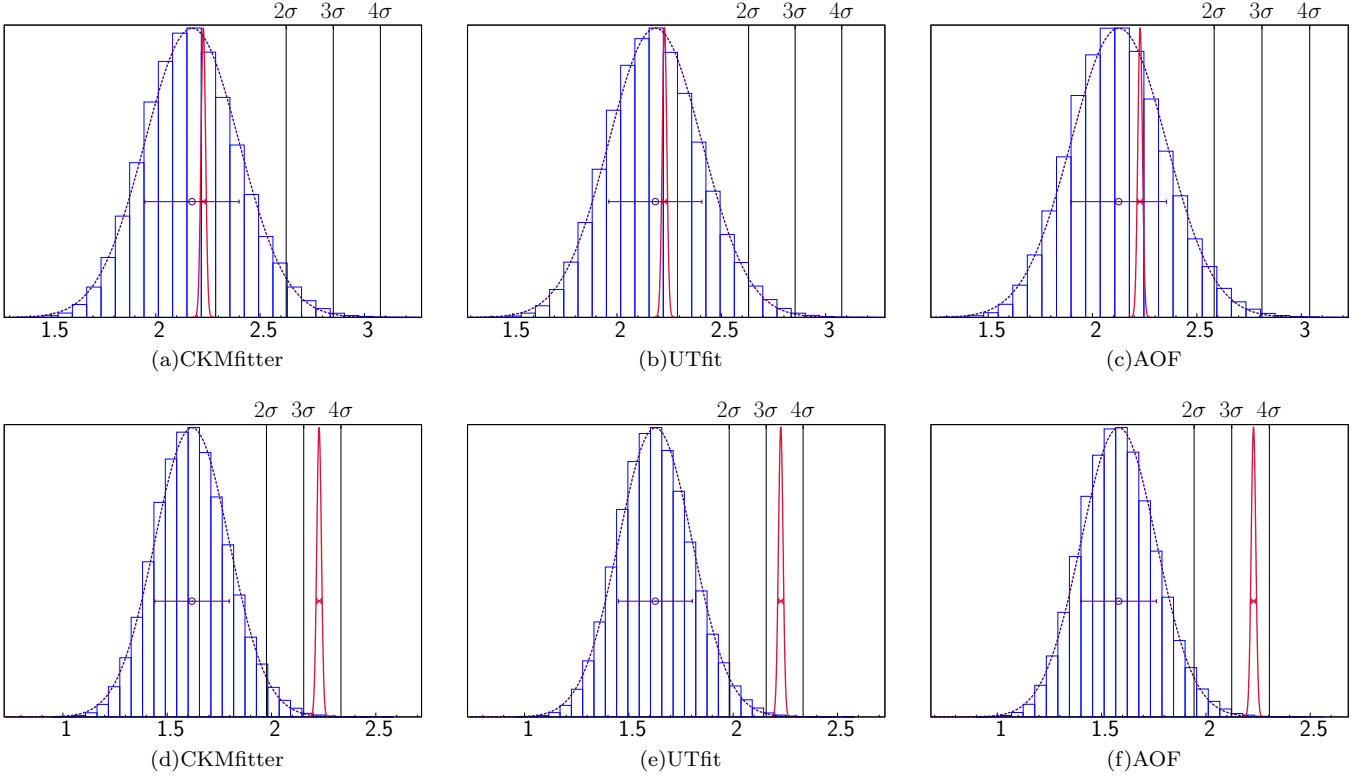


FIG. 2. Gaussian probability distributions for $\varepsilon_K^{\text{SM}}$ (blue dotted line) and $\varepsilon_K^{\text{Exp}}$ (red solid line). Here, the results are obtained using the FLAG \hat{B}_K . The results of 2(a), 2(b), and 2(c) are obtained using the inclusive V_{cb} . Those of 2(d), 2(e), and 2(f) are obtained using the exclusive V_{cb} .

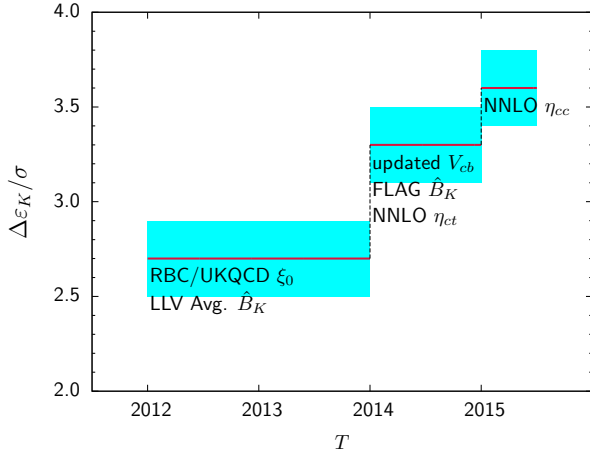


FIG. 3. Recent history of $\Delta\varepsilon_K$ along with the theoretical progress. The blue band represents the systematic error.

sive channel. Using the FLAG average for \hat{B}_K [10] and the NNLO value of η_{ct} [51], the SWME collaboration reported the updated $\Delta\varepsilon_K = 3.3(2)\sigma$ in Ref. [53] in 2014. In this paper, we investigate issues in the NNLO calculation of η_{cc} [52, 54] and use the SWME result in Table V to report the updated $\Delta\varepsilon_K = 3.6(2)\sigma$ in Eq. (87).

V. CONCLUSION

In this paper, we observe that there is a substantial $3.6(2)\sigma$ tension in ε_K between experiment and the SM theory with lattice QCD inputs. For this claim, we choose the angle-only fit (AOF), the exclusive V_{cb} (lattice QCD results), and the FLAG \hat{B}_K (lattice QCD results) to determine the central value. The systematic uncertainty is obtained by taking the maximum deviation from the central value by choosing other input parameters from the global fits of CKMfitter and UTfit. We choose the AOF method to determine the central value because the AOF Wolfenstein parameters do not have unwanted correlation with ε_K and \hat{B}_K . However, the tension disappears in the case of inclusive V_{cb} (results of the heavy quark expansion based on the OPE) regardless of the choices for the Wolfenstein parameters.

In Table IX, we present the error budget of $\varepsilon_K^{\text{SM}}$ for the central value. This is obtained using the error propagation method explained in Section III B. From this error budget, we find out that V_{cb} dominates the error in $\varepsilon_K^{\text{SM}}$. Hence, it is essential to reduce the error of V_{cb} as much as possible. (See also Refs. [60, 61].) In order to achieve this goal, we plan to extract V_{cb} from the exclusive channel using the Oktay-Kronfeld (OK) action [62] for heavy quarks to calculate the form factors for $\bar{B} \rightarrow D^{(*)}\ell\bar{\nu}$ de-

TABLE IX. Error budget for $\varepsilon_K^{\text{SM}}$ obtained using the AOF method, the exclusive V_{cb} , and the FLAG \hat{B}_K . Here, the values are fractional contributions to the total error obtained using the formula in Eq. (85).

source	error (%)	memo
V_{cb}	40.7	FNAL/MILC
$\bar{\eta}$	21.0	AOF
η_{ct}	17.2	$c-t$ Box
η_{cc}	7.3	$c-c$ Box
$\bar{\rho}$	4.7	AOF
m_t	2.5	
ξ_0	2.2	RBC/UKQCD
\hat{B}_K	1.6	FLAG
m_c	1.0	
\vdots	\vdots	

cays. Preliminary results in the early stage of the V_{cb} project are reported in Refs. [63–65].

Our work on η_{cc} are consistent with the conclusion of Ref. [52] regarding the convergence of perturbation theory. The uncertainty due to truncating the expansion remains an important question for future work. Lattice QCD calculations with dynamical charm quarks, such as that envisioned by the RBC/UKQCD collaboration, could shed light on this issue.

We expect that our results for ε_K would be consistent with those from a global UT analysis, such as that in Ref. [58]. Such a global analysis with up-to-date inputs from lattice QCD has not been performed yet. It would be interesting to see the results of such an analysis.

ACKNOWLEDGMENTS

Y.C.J. thanks to Amarjit Soni for helpful discussion on the unitarity triangle analysis. We thank to J. Brod and A. J. Buras for a useful discussion on the η_{cc} . The research of W. Lee is supported by the Creative Research Initiatives Program (No. 2014001852) of the NRF grant funded by the Korean government (MEST). W. Lee would like to acknowledge the support from the KISTI supercomputing center through the strategic support program for the supercomputing application research [No. KSC-2014-G3-002]. Computations were carried out on the DAVID GPU clusters at Seoul National University. J.A.B. is supported by the Basic Science Research Program of the National Research Foundation of Korea (NRF) funded by the Ministry of Education (No. 2014027937).

Appendix A: Next-to-next-to leading order η_{cc}

We will begin from the master formula for η_{cc} [52] and give an explicit expression for each component which is

necessary for a numerical evaluation. For $\mu \leq \mu_c$,

$$\eta_{cc} = \frac{1}{m_c^2(m_c)} \tilde{C}_{S2}^{cc}(\mu_c) [\alpha_s(\mu_c, 3)]^{a_+(3)} K_+^{-1}(\mu_c, 3). \quad (\text{A1})$$

The magic number $a_+(3) = 2/9$ can be obtained from Eq. (A32). $\alpha_s(\mu, f)$ is the running strong coupling constant with f active flavors at scale μ . We will use the four-loop α_s running formula [40, 66]. The Wilson coefficient $\tilde{C}_{S2}^{cc}(\mu_c)$ of the $\Delta S = 2$ four-fermion operator is defined by Eq. (A2). The running matrix $K_+^{-1}(\mu_c, 3)$ is given by Eq. (A29).

At the charm scale μ_c , the effective four flavor theory is matched to the effective three flavor theory by requiring the following condition [52],

$$\sum_{i,j=+,-} C_i C_j \langle Q_i Q_j \rangle = \frac{1}{8\pi^2} \tilde{C}_{S2}^{cc} \langle \tilde{Q}_{S2} \rangle. \quad (\text{A2})$$

The matrix elements and the Wilson coefficients are expanded in the three flavor strong coupling $\alpha_s(\mu_c, 3)$,

$$\langle \tilde{Q}_{S2} \rangle = \tilde{r}_{S2} \langle \tilde{Q}_{S2} \rangle^{(0)}, \quad (\text{A3})$$

$$\tilde{r}_{S2} = 1 + \frac{\alpha_s(\mu_c, 3)}{4\pi} \tilde{r}_{S2}^{(1)} + \left(\frac{\alpha_s(\mu_c, 3)}{4\pi} \right)^2 \tilde{r}_{S2}^{(2)}, \quad (\text{A4})$$

$$\langle Q_i Q_j \rangle = \frac{m_c^2(\mu_c)}{8\pi^2} d_{ij} \langle \tilde{Q}_{S2} \rangle^{(0)}, \quad (\text{A5})$$

$$d_{ij} = d_{ij}^{(0)} + \frac{\alpha_s(\mu_c, 3)}{4\pi} d_{ij}^{(1)} + \left(\frac{\alpha_s(\mu_c, 3)}{4\pi} \right)^2 d_{ij}^{(2)}, \quad (\text{A6})$$

$$C_i(\mu_c) = C_i^{(0)}(\mu_c) + \frac{\alpha_s(\mu_c, 3)}{4\pi} C_i^{(1)}(\mu_c) + \left(\frac{\alpha_s(\mu_c, 3)}{4\pi} \right)^2 C_i^{(2)}(\mu_c), \quad (\text{A7})$$

$$\tilde{C}_{S2}^{cc}(\mu_c) = \tilde{C}_{S2}^{cc(0)}(\mu_c) + \frac{\alpha_s(\mu_c, 3)}{4\pi} \tilde{C}_{S2}^{cc(1)}(\mu_c) + \left(\frac{\alpha_s(\mu_c, 3)}{4\pi} \right)^2 \tilde{C}_{S2}^{cc(2)}(\mu_c). \quad (\text{A8})$$

Then, the matching results are

$$\tilde{C}_{S2}^{cc(0)}(\mu_c) = m_c^2(\mu_c) C_i^{(0)} C_j^{(0)} d_{ij}^{(0)}, \quad (\text{A9})$$

$$\tilde{C}_{S2}^{cc(1)}(\mu_c) = m_c^2(\mu_c) \left[C_i^{(0)} C_j^{(0)} \hat{d}_{ij}^{(1)} + (C_i^{(1)} C_j^{(0)} + C_i^{(0)} C_j^{(1)}) d_{ij}^{(0)} \right], \quad (\text{A10})$$

$$\begin{aligned} \tilde{C}_{S2}^{cc(2)}(\mu_c) = m_c^2(\mu_c) & \left[C_i^{(0)} C_j^{(0)} \left(\hat{d}_{ij}^{(2)} + \frac{2}{3} \log \frac{\mu_c^2}{m_c^2} d_{ij}^{(1)} \right) \right. \\ & + (C_i^{(1)} C_j^{(0)} + C_i^{(0)} C_j^{(1)}) \left(\hat{d}_{ij}^{(1)} + \frac{2}{3} \log \frac{\mu_c^2}{m_c^2} d_{ij}^{(0)} \right) \\ & \left. + (C_i^{(2)} C_j^{(0)} + C_i^{(1)} C_j^{(1)} + C_i^{(0)} C_j^{(2)}) d_{ij}^{(0)} \right], \quad (\text{A11}) \end{aligned}$$

where $m_c = m_c(m_c)$ in the logarithms multiplied by $d_{ij}^{(0,1)}$, and

$$\hat{d}_{ij}^{(1)} \equiv d_{ij}^{(1)} - d_{ij}^{(0)} \tilde{r}_{S_2}^{(1)}, \quad (\text{A12})$$

$$\hat{d}_{ij}^{(2)} \equiv d_{ij}^{(2)} - \hat{d}_{ij}^{(1)} \tilde{r}_{S_2}^{(1)} - d_{ij}^{(0)} \tilde{r}_{S_2}^{(2)}. \quad (\text{A13})$$

Note that the matching scale is the charm quark mass $\mu_c = m_c(m_c)$; in Eqs. (A9), (A10), and (A11), the Wilson coefficients $C_i^{(l)}(\mu_c)$ ($l = 0, 1, 2; i = \pm$) are evaluated at $\mu_c = m_c$,

$$C_i^{(l)} = C_i^{(l)}(m_c). \quad (\text{A14})$$

These are obtained by renormalization group evolution from the scale μ_W down to the scale $\mu_c = m_c$. (See Eq. (A45).) To examine the size of residual scale dependence, we vary μ_c , keeping the condition Eq. (A14).

Then the residual scale μ_c dependence in $\tilde{C}_{S_2}^{(l)}(\mu_c)$ enters from logarithms which are shown explicitly in Eq. (A11) and through $d_{ij}^{(l)}$ and $\tilde{r}_{S_2}^{(l)}$; it also comes from the expansion $m_c(\mu_c)$. The expansion of the charm quark mass $m_c(\mu_c)$ near $\mu_c = m_c$ is given by Eq. (A48) with $f = 4$. The resulting residual scale dependence in η_{cc} can be seen from Fig. 4.

The leading and next-to-leading order (NLO) calculations can be found from Ref. [67], with the number of colors $N_c = 3$, $l_c = \log(\mu_c^2/m_c^2(\mu_c))$,

$$\begin{aligned} d_{+++}^{(0)} &= \frac{3}{2}, \\ d_{+-}^{(0)} = d_{-+}^{(0)} &= -\frac{1}{2}, \\ d_{--}^{(0)} &= \frac{1}{2}, \end{aligned} \quad (\text{A15})$$

$$\begin{aligned} d_{+++}^{(1)} &= 9l_c - \frac{27}{2} - \frac{\pi^2}{6}, \\ d_{+-}^{(1)} = d_{-+}^{(1)} &= -6l_c - \frac{23}{6} + \frac{5\pi^2}{18}, \\ d_{--}^{(1)} &= 6l_c + \frac{53}{6} + \frac{\pi^2}{18}, \end{aligned} \quad (\text{A16})$$

$$\tilde{r}_{S_2}^{(1)} = -\frac{17}{3}. \quad (\text{A17})$$

The next-to-next-to-leading order (NNLO) calculation results are presented in Ref. [52],

$$\begin{aligned} \hat{d}_{+++}^{(2)} &= \frac{1665873233}{8164800} - \frac{1573}{162} B_4 - \frac{133}{72} D_3 \\ &+ \frac{49}{36} \zeta_2 l_c + \frac{4313}{216} l_c^2 - \frac{15059}{1296} l_c \\ &+ \frac{210213}{560} S_2 - \frac{1501}{54} \zeta_2^2 - \frac{7567241}{204120} \zeta_2 \\ &- \frac{1697893}{7776} \zeta_3 + \frac{11575}{216} \zeta_4, \end{aligned} \quad (\text{A18})$$

$$\begin{aligned} \hat{d}_{+-}^{(2)} = \hat{d}_{-+}^{(2)} &= \frac{87537463}{1166400} + \frac{685}{162} B_4 - \frac{83}{72} D_3 \\ &+ \frac{695}{36} \zeta_2 l_c - \frac{1475}{216} l_c^2 - \frac{57763}{1296} l_c \\ &- \frac{4797}{80} S_2 - \frac{791}{54} \zeta_2^2 + \frac{366569}{29160} \zeta_2 \\ &+ \frac{57673}{7776} \zeta_3 - \frac{4999}{216} \zeta_4, \end{aligned} \quad (\text{A19})$$

$$\begin{aligned} \hat{d}_{--}^{(2)} &= \frac{2129775941}{8164800} + \frac{491}{162} B_4 + \frac{11}{72} D_3 \\ &+ \frac{865}{36} \zeta_2 l_c + \frac{12533}{216} l_c^2 + \frac{171121}{1296} l_c \\ &+ \frac{59121}{560} S_2 - \frac{517}{54} \zeta_2^2 + \frac{9261883}{204120} \zeta_2 \\ &- \frac{411709}{7776} \zeta_3 - \frac{7913}{216} \zeta_4. \end{aligned} \quad (\text{A20})$$

Some constants for the master integrals are [68]

$$\begin{aligned} D_3 &= 6\zeta_3 - \frac{15}{4} \zeta_4 - 6 \left[\text{Cl}_2 \left(\frac{\pi}{3} \right) \right]^2, \\ B_4 &= -4\zeta_2 \ln^2 2 + \frac{2}{3} \ln^4 2 - \frac{13}{2} \zeta_4 + 16 \text{Li}_4 \left(\frac{1}{2} \right), \\ S_2 &= \frac{4}{9\sqrt{3}} \text{Cl}_2 \left(\frac{\pi}{3} \right), \end{aligned} \quad (\text{A21})$$

with

$$\text{Cl}_2(x) = \text{Im} \left(\text{Li}_2(e^{ix}) \right), \quad (\text{A22})$$

$$\text{Li}_n(z) = \sum_{k=1}^{\infty} \frac{z^k}{k^n}, \quad (\text{A23})$$

and the Riemann zeta function is

$$\zeta_n = \sum_{k=1}^{\infty} \frac{1}{k^n}. \quad (\text{A24})$$

In numerical evaluation, we use approximated numbers which are obtained using `Mathematica`.

$$\begin{aligned} \zeta_2 &= 1.644934 \dots = \frac{\pi^2}{6}, \\ \zeta_3 &= 1.202056 \dots, \\ \zeta_4 &= 1.082323 \dots = \frac{\pi^4}{90}, \\ \text{Li}_4 \left(\frac{1}{2} \right) &= 0.5174790 \dots, \\ \text{Cl}_2 \left(\frac{\pi}{3} \right) &= 1.014941 \dots \end{aligned} \quad (\text{A25})$$

For ζ_2 and ζ_4 , we also give the exact expression.

The renormalization group evolution of the Wilson coefficients C_{\pm} is described by the evolution matrix U_{ij} [69],

$$C_i(\mu) = U_{ij}(\mu, \mu_0) C_j(\mu_0), \quad (\text{A26})$$

which is diagonalized by the specific choice of evanescent operators,

$$U_{ij}(\mu, \mu_0) = K_i(\mu) \left(\frac{\alpha_s(\mu_0, f)}{\alpha_s(\mu, f)} \right)^{a_i} K_i^{-1}(\mu_0) \delta_{ij}, \quad (\text{A27})$$

where

$$K_{\pm}(\mu) = 1 + \frac{\alpha_s(\mu, f)}{4\pi} J_{\pm}^{(1)} + \left(\frac{\alpha_s(\mu, f)}{4\pi} \right)^2 J_{\pm}^{(2)}, \quad (\text{A28})$$

$$K_{\pm}^{-1}(\mu_0) = 1 - \frac{\alpha_s(\mu_0, f)}{4\pi} J_{\pm}^{(1)} - \left(\frac{\alpha_s(\mu_0, f)}{4\pi} \right)^2 (J_{\pm}^{(2)} - (J_{\pm}^{(1)})^2), \quad (\text{A29})$$

and

$$J_{\pm}^{(1)} = \frac{\beta_1}{\beta_0} a_{\pm} - \frac{\gamma_{\pm}^{(1)}}{2\beta_0}, \quad (\text{A30})$$

$$J_{\pm}^{(2)} = \frac{\beta_2}{2\beta_0} a_{\pm} + \frac{1}{2} \left((J_{\pm}^{(1)})^2 - \frac{\beta_1}{\beta_0} J_{\pm}^{(1)} \right) - \frac{\gamma_{\pm}^{(2)}}{4\beta_0}. \quad (\text{A31})$$

The expansion coefficients of the QCD beta function β_i are given in Eq. (A46). The anomalous dimensions $\gamma_{\pm}^{(i)}$ for the operators Q_{\pm} are taken from Ref. [70],

$$\gamma_{\pm}^{(0)} = \pm 6 \left(1 \mp \frac{1}{3} \right) = 2\beta_0 a_{\pm}, \quad (\text{A32})$$

$$\gamma_{\pm}^{(1)} = \left(-\frac{21}{2} \pm \frac{2}{3} f \right) \left(1 \mp \frac{1}{3} \right), \quad (\text{A33})$$

$$\gamma_{\pm}^{(2)} = \frac{1}{300} (349049 \pm 201485) - \frac{1}{1350} (115577 \mp 9795) f \mp \frac{130}{27} \left(1 \mp \frac{1}{3} \right) f^2 \mp \left(672 + 80 \left(1 \mp \frac{1}{3} \right) f \right) \zeta_3. \quad (\text{A34})$$

The number of active flavors is fixed while applying Eq. (A26). The number of flavors is implied by the strong coupling constant in Eq. (A27).

The initial conditions for the Wilson coefficients C_{\pm} are chosen at the scale μ_W ,

$$C_{\pm}(\mu_W) = C_{\pm}^{(0)}(\mu_W) + \frac{\alpha_s(\mu_W, 5)}{4\pi} C_{\pm}^{(1)}(\mu_W) + \left(\frac{\alpha_s(\mu_W, 5)}{4\pi} \right)^2 C_{\pm}^{(2)}(\mu_W). \quad (\text{A35})$$

The expansion coefficients are given in Ref. [70],

$$\begin{aligned} C_{\pm}^{(0)}(\mu_W) &= 1, \\ C_{\pm}^{(1)}(\mu_W) &= \pm \frac{1}{2} \left(1 \mp \frac{1}{3} \right) \left(11 + 6 \ln \frac{\mu_W^2}{M_W^2} \right), \\ C_{\pm}^{(2)}(\mu_W) &= -\frac{1}{3600} (135677 \mp 124095) \\ &\quad + \frac{1}{18} (7 \pm 51) \pi^2 \mp \frac{1}{2} \left(1 \mp \frac{1}{3} \right) T(x_t) \end{aligned}$$

$$- \frac{5}{36} (11 \mp 249) \ln \frac{\mu_W^2}{M_W^2} + \frac{1}{6} (7 \pm 51) \ln^2 \frac{\mu_W^2}{M_W^2}, \quad (\text{A36})$$

where

$$\begin{aligned} T(x_t) &= \frac{112}{9} + 32x_t + \left(\frac{20}{3} + 16x_t \right) \ln x_t \\ &\quad - (8 + 16x_t) \sqrt{4x_t - 1} \text{Cl}_2 \left(2 \arcsin \left(\frac{1}{2\sqrt{x_t}} \right) \right), \end{aligned} \quad (\text{A37})$$

$x_t = m_t^2(\mu_W)/M_W^2$, and $\text{Cl}_2(x)$ is given in Eq. (A22).

In numerical evaluation, we use an approximated number which is obtained using *Mathematica*,

$$\text{Cl}_2 \left(2 \arcsin \left(\frac{1}{2\sqrt{x_t}} \right) \right) = 0.8464504 \dots \quad (\text{A38})$$

The value x_t is evaluated with the top quark mass $m_t(m_t) = 163.3$ GeV and $M_W = 80.385$ GeV, approximating $m_t(\mu_W) = m_t(m_t)$.

Running from μ_W to the bottom quark threshold μ_b is achieved by

$$\begin{aligned} C_i(\mu_b, 5) &= K_i(\mu_b, 5) \left(\frac{\alpha_s(\mu_W, 5)}{\alpha_s(\mu_b, 5)} \right)^{a_i(5)} K_i^{-1}(\mu_W, 5) C_i(\mu_W) \\ &= C_i^{(0)}(\mu_b, 5) + \frac{\alpha_s(\mu_b, 5)}{4\pi} C_i^{(1)}(\mu_b, 5) \\ &\quad + \left(\frac{\alpha_s(\mu_b, 5)}{4\pi} \right)^2 C_i^{(2)}(\mu_b, 5). \end{aligned} \quad (\text{A39})$$

The threshold correction at μ_b is given by the following. Writing

$$\begin{aligned} C_i(\mu_b, 4) &= C_i^{(0)}(\mu_b, 4) + \frac{\alpha_s(\mu_b, 4)}{4\pi} C_i^{(1)}(\mu_b, 4) \\ &\quad + \left(\frac{\alpha_s(\mu_b, 4)}{4\pi} \right)^2 C_i^{(2)}(\mu_b, 4), \end{aligned} \quad (\text{A40})$$

then

$$\begin{aligned} C_i^{(0)}(\mu_b, 4) &= C_i^{(0)}(\mu_b, 5), \\ C_i^{(1)}(\mu_b, 4) &= C_i^{(1)}(\mu_b, 5), \\ C_i^{(2)}(\mu_b, 4) &= C_i^{(2)}(\mu_b, 5) - \delta C_i^{(2)}(\mu_b), \end{aligned} \quad (\text{A41})$$

where

$$\begin{aligned} \delta C_{\pm}^{(2)}(\mu_b) &= -\frac{2}{3} \ln \frac{\mu_b^2}{m_b^2} C_{\pm}^{(1)}(\mu_b, 5) \\ &\quad - \left(\frac{2}{3} \ln \frac{\mu_b^2}{m_b^2} r_{\pm}^{(1)}(\mu_b, 5) + \delta r_{\pm}^{(2)}(\mu_b) \right) C_{\pm}^{(0)}(\mu_b, 5) \\ &= -\frac{2}{3} \ln \frac{\mu_b^2}{m_b^2} C_{\pm}^{(1)}(\mu_b, 5) \\ &\quad + \left(\pm \left(1 \mp \frac{1}{3} \right) \left(\frac{59}{36} + \frac{1}{3} \ln \frac{\mu_b^2}{m_b^2} + \ln^2 \frac{\mu_b^2}{m_b^2} \right) \right) C_{\pm}^{(0)}(\mu_b, 5). \end{aligned} \quad (\text{A42})$$

The definition of $r_i^{(1)}$ and $\delta r_i^{(2)}$, and their combination, the multiplicative factor of $C_i^{(0)}$, can be found in Ref. [70].

Running from μ_b to the matching scale $\mu_c = m_c(m_c)$ is achieved by

$$\begin{aligned} C_i(\mu_c, 4) &= K_i(\mu_c, 4) \left(\frac{\alpha_s(\mu_b, 4)}{\alpha_s(\mu_c, 4)} \right)^{\alpha_i(4)} K_i^{-1}(\mu_b, 4) C_i(\mu_b, 4) \\ &= C_i^{(0)}(\mu_c, 4) + \frac{\alpha_s(\mu_c, 4)}{4\pi} C_i^{(1)}(\mu_c, 4) \\ &\quad + \left(\frac{\alpha_s(\mu_c, 4)}{4\pi} \right)^2 C_i^{(2)}(\mu_c, 4). \end{aligned} \quad (\text{A43})$$

In the matching calculation, we need the expansion in the three flavor strong coupling, Eq. (A7).

Equating $C_i(\mu_c)$ in Eq. (A7) to $C_i(\mu_c, 4)$ after applying Eq. (A47) to the flavor threshold with $f = 4$, then

$$\begin{aligned} C_i^{(0)}(\mu_c) &= C_i^{(0)}(\mu_c, 4), \\ C_i^{(1)}(\mu_c) &= C_i^{(1)}(\mu_c, 4), \\ C_i^{(2)}(\mu_c) &= C_i^{(2)}(\mu_c, 4) + \frac{2}{3} \ln \frac{\mu_c^2}{m_c^2} C_i^{(1)}(\mu_c, 4). \end{aligned} \quad (\text{A44})$$

Hence, at the matching scale of the charm quark mass $\mu_c = m_c(m_c)$, we obtain

$$C_i^{(l)}(m_c) = C_i^{(l)}(m_c, 4), \quad (l = 0, 1, 2). \quad (\text{A45})$$

The QCD beta function expansion coefficients β_i to four-loop order are [40, 70]:

$$\begin{aligned} \beta_0 &= 11 - \frac{2}{3}f, \\ \beta_1 &= 102 - \frac{38}{3}f, \\ \beta_2 &= \frac{2857}{2} - \frac{5033}{18}f + \frac{325}{54}f^2, \\ \beta_3 &= \frac{149753}{6} + 3564\zeta_3 - \left(\frac{1078361}{162} + \frac{6508}{27}\zeta_3 \right) f \\ &\quad + \left(\frac{50065}{162} + \frac{6472}{81}\zeta_3 \right) f^2 + \frac{1093}{729}f^3. \end{aligned} \quad (\text{A46})$$

The NNNLO decoupling relation of the strong coupling constant at a flavor threshold μ is [40]

$$\begin{aligned} &\frac{\alpha_s(\mu, f-1)}{4\pi} \\ &= \frac{\alpha_s(\mu, f)}{4\pi} - \left(\frac{\alpha_s(\mu, f)}{4\pi} \right)^2 \frac{2}{3} \ln \frac{\mu^2}{m_h^2} \\ &\quad + \left(\frac{\alpha_s(\mu, f)}{4\pi} \right)^3 \left(\frac{22}{9} - \frac{38}{3} \ln \frac{\mu^2}{m_h^2} + \frac{4}{9} \ln^2 \frac{\mu^2}{m_h^2} \right) \\ &\quad + \left(\frac{\alpha_s(\mu, f)}{4\pi} \right)^4 \left(\frac{564731}{1944} - \frac{2633}{486}(f-1) - \frac{82043}{432}\zeta_3 \right) \\ &\quad + \frac{1}{27} \ln \frac{\mu^2}{m_h^2} (-6793 + 281(f-1)) \end{aligned}$$

$$- \frac{131}{9} \ln^2 \frac{\mu^2}{m_h^2} - \frac{8}{27} \ln^3 \frac{\mu^2}{m_h^2} \Big), \quad (\text{A47})$$

where $m_h = m_h(m_h)$ is the scale invariant $\overline{\text{MS}}$ mass of the heavy flavor which is removed from an effective theory below the threshold μ , and ζ_3 is a Riemann zeta function, Eq. (A24).

The running quark mass $m_q(\mu)$, an $\overline{\text{MS}}$ mass at scale μ , for a fixed number of active flavors f is [40]

$$\frac{m_q(\mu)}{m_q(\mu_0)} = \frac{R(\alpha_s(\mu)/4\pi)}{R(\alpha_s(\mu_0)/4\pi)}, \quad (\text{A48})$$

with

$$\begin{aligned} R(x) &= x^{c_0} \left\{ 1 + (c_1 - b_1 c_0)x \right. \\ &\quad + \frac{1}{2} [(c_1 - b_1 c_0)^2 + c_2 - b_1 c_1 + b_1^2 c_0 - b_2 c_0] x^2 \\ &\quad + \left[\frac{1}{6}(c_1 - b_1 c_0)^3 \right. \\ &\quad + \frac{1}{2}(c_1 - b_1 c_0)(c_2 - b_1 c_1 + b_1^2 c_0 - b_2 c_0) \\ &\quad + \frac{1}{3}(c_3 - b_1 c_2 + b_1^2 c_1 - b_2 c_1 - b_1^3 c_0 \\ &\quad \left. \left. + 2b_1 b_2 c_0 - b_3 c_0) \right] x^3 \right\}, \end{aligned} \quad (\text{A49})$$

where $m_q(\mu_0)$ is the scale invariant mass $m_q = m_q(m_q)$, $b_i = \beta_i/\beta_0$, and $c_i = \gamma_m^{(i)}/\beta_0$. The QCD beta function coefficients β_i are given in Eq. (A46). The mass anomalous dimensions $\gamma_m^{(i)}$ are known up to four-loop order,

$$\begin{aligned} \gamma_m^{(0)} &= 4, \\ \gamma_m^{(1)} &= \frac{202}{3} - \frac{20}{9}f, \\ \gamma_m^{(2)} &= 1249 - \left(\frac{2216}{27} + \frac{160}{3}\zeta_3 \right) f - \frac{140}{81}f^2, \\ \gamma_m^{(3)} &= \frac{4603055}{162} + \frac{135680}{27}\zeta_3 - 8800\zeta_5 \\ &\quad + \left(-\frac{91723}{27} - \frac{34192}{9}\zeta_3 + 880\zeta_4 + \frac{18400}{9}\zeta_5 \right) f \\ &\quad + \left(\frac{5242}{243} + \frac{800}{9}\zeta_3 - \frac{160}{3}\zeta_4 \right) f^2 + \left(-\frac{332}{243} + \frac{64}{27}\zeta_3 \right) f^3. \end{aligned} \quad (\text{A50})$$

In numerical evaluation, we use approximated numbers for the Riemann zeta functions ζ_n which are obtained using *Mathematica*,

$$\zeta_5 = 1.036927\dots, \quad (\text{A51})$$

and ζ_3 and ζ_4 are given in Eq. (A25).

We used Eq. (A48) to expand the charm quark mass about $m_c = m_c(m_c)$ with $f = 4$.

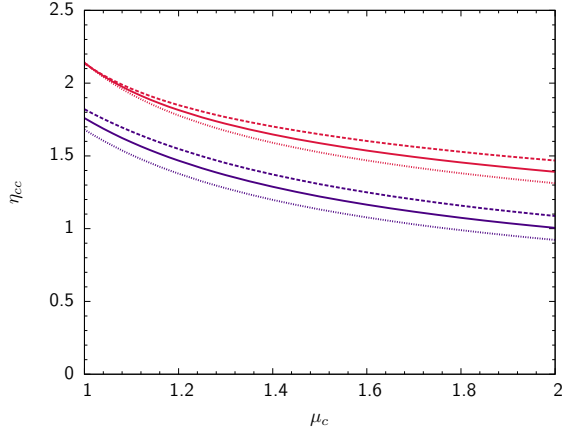


FIG. 4. Scale μ_c dependence of η_{cc} . Dotted, solid, and dashed lines represent results for $\mu_W = 40, 80,$ and 160 GeV, respectively. The upper three (red) lines are the NNLO results, and the lower three (purple) lines are the NLO results.

Here, we will give numerical results for an initial scale $\mu_W = 80$ GeV and a varying charm scale μ_c , $1.0 \leq \mu_c \leq 2.0$ GeV. To examine the dependence on the scale μ_W , we repeat the same analysis with $\mu_W = 40, 160$ GeV. The dependence on μ_b and $m_t(m_t)$ is ignored [52]. Fig. 4 summarizes these results. The following are kept fixed for all analyses: the gauge boson masses $M_Z = 91.1876$ GeV, $M_W = 80.385$ GeV; quark masses $m_t(m_t) = 163.3$ GeV, $m_b(m_b) = 4.163$ GeV, $m_c(m_c) = 1.279$ GeV; bottom quark threshold $\mu_b = 5.0$ GeV; and the strong coupling constant that provides an initial value for the running formula, $\alpha_s(M_Z, 5) = 0.1184$ GeV.

At the scales $\mu_W = 80$ GeV and $\mu_c = 1.279$ GeV,

$$\begin{aligned} \eta_{cc}/[\alpha_s(\mu_c, 3)]^{a+} &= 1.129757 + 0.571608 + 0.430890, \\ \eta_{cc}^{\text{NNLO}} &= 1.738396, \\ \eta_{cc}^{\text{NLO}} &= 1.387098. \end{aligned} \quad (\text{A52})$$

The value of η_{cc}^{NLO} is obtained by summing the first two terms in the series, and the value of η_{cc}^{NNLO} is obtained by summing all three terms in the series.

At the scales $\mu_W = 80$ GeV and $\mu_c = 1.300$ GeV,

$$\begin{aligned} \eta_{cc}/[\alpha_s(\mu_c, 3)]^{a+} &= 1.113769 + 0.568911 + 0.433783, \\ \eta_{cc}^{\text{NNLO}} &= 1.720690, \\ \eta_{cc}^{\text{NLO}} &= 1.368023. \end{aligned} \quad (\text{A53})$$

We claim the NNLO η_{cc} is

$$\eta_{cc}^{\text{NNLO}} = 1.72(27). \quad (\text{A54})$$

The central value corresponds to the result with the scales $\mu_c = 1.3$ GeV and $\mu_W = 80$ GeV. For the error, we add the μ_c and μ_W dependences in quadrature,

$$\begin{aligned} \delta_{\mu_c} &= \eta_{cc}^{\text{NNLO}}(\mu_c = 1.3 \text{ GeV}, \mu_W = 80 \text{ GeV}) \\ &\quad - \eta_{cc}^{\text{NNLO}}(\mu_c = 1.8 \text{ GeV}, \mu_W = 80 \text{ GeV}) \end{aligned}$$

$$= 0.266,$$

$$\begin{aligned} \delta_{\mu_W} &= (\eta_{cc}^{\text{NNLO}}(\mu_c = 1.3 \text{ GeV}, \mu_W = 160 \text{ GeV}) \\ &\quad - \eta_{cc}^{\text{NNLO}}(\mu_c = 1.3 \text{ GeV}, \mu_W = 40 \text{ GeV}))/2 \\ &= 0.047. \end{aligned} \quad (\text{A55})$$

Though we include errors from the inputs $\alpha_s(M_Z, 5)$ and $m_c(m_c)$, the final errors in Eq. (A54) are not affected; we use the errors quoted in Ref. [52]:

$$\delta_{\alpha_s} = 0.06, \quad \delta_{m_c} = 0.01. \quad (\text{A56})$$

In Ref. [52], the authors also added the absolute shift from the NLO value of η_{cc} . It is the main reason for their larger error,

$$\eta_{cc}^{\text{NNLO}} = 1.87(76). \quad (\text{A57})$$

The main concern for adding this shift is poor convergence of the α_s expansion for η_{cc} . We, however, take the view that the error from μ_c dependence suffices to estimate the size of higher order corrections.

Our result is close to the value quoted in Ref. [54]

$$\eta_{cc} \approx 1.70(21). \quad (\text{A58})$$

Our result for η_{cc}^{NLO} agrees with the value quoted in Ref. [52]

$$\eta_{cc}^{\text{NLO}} = 1.38(52)(07)(02). \quad (\text{A59})$$

Appendix B: $\varepsilon_K^{\text{SM}}$ with the SWME \hat{B}_K

Lattice results for the exclusive V_{cb} [18] and the SWME \hat{B}_K [16] are obtained using overlapping subsets of the MILC asqtad gauge ensembles [47]. This implies that there exists a complicated, non-trivial correlation between them. It is possible to calculate, in principle, this correlation exactly from the data set. Unfortunately, this correlation is not available yet. Hence, the current situation is that we need to estimate the systematic error due to the unknown correlation between \hat{B}_K and V_{cb} .

Here is our strategy. First, we take the uncorrelated case as the central value. Second, we introduce +50% correlation between \hat{B}_K and V_{cb} and obtain results for $\varepsilon_K^{\text{SM}}$. Third, we introduce -50% anti-correlation between \hat{B}_K and V_{cb} and repeat the analysis to obtain $\varepsilon_K^{\text{SM}}$. Fourth, we take the maximum deviation from the central value as the systematic error due to the unknown correlation between \hat{B}_K and V_{cb} .

In Table X, we present results for $\varepsilon_K^{\text{SM}}$ for the uncorrelated case. In Table XI, we present the corresponding results for $\Delta\varepsilon_K$. In Fig. 5, we show the corresponding probability distribution of $\varepsilon_K^{\text{SM}}$.

In Table XII, we present results for $\varepsilon_K^{\text{SM}}$ with +50% correlation and -50% anti-correlation between \hat{B}_K and (exclusive) V_{cb} . In Table XIII, we present the corresponding results for $\Delta\varepsilon_K$. In Fig. 6, we show the probability distribution for the corresponding $\varepsilon_K^{\text{SM}}$.

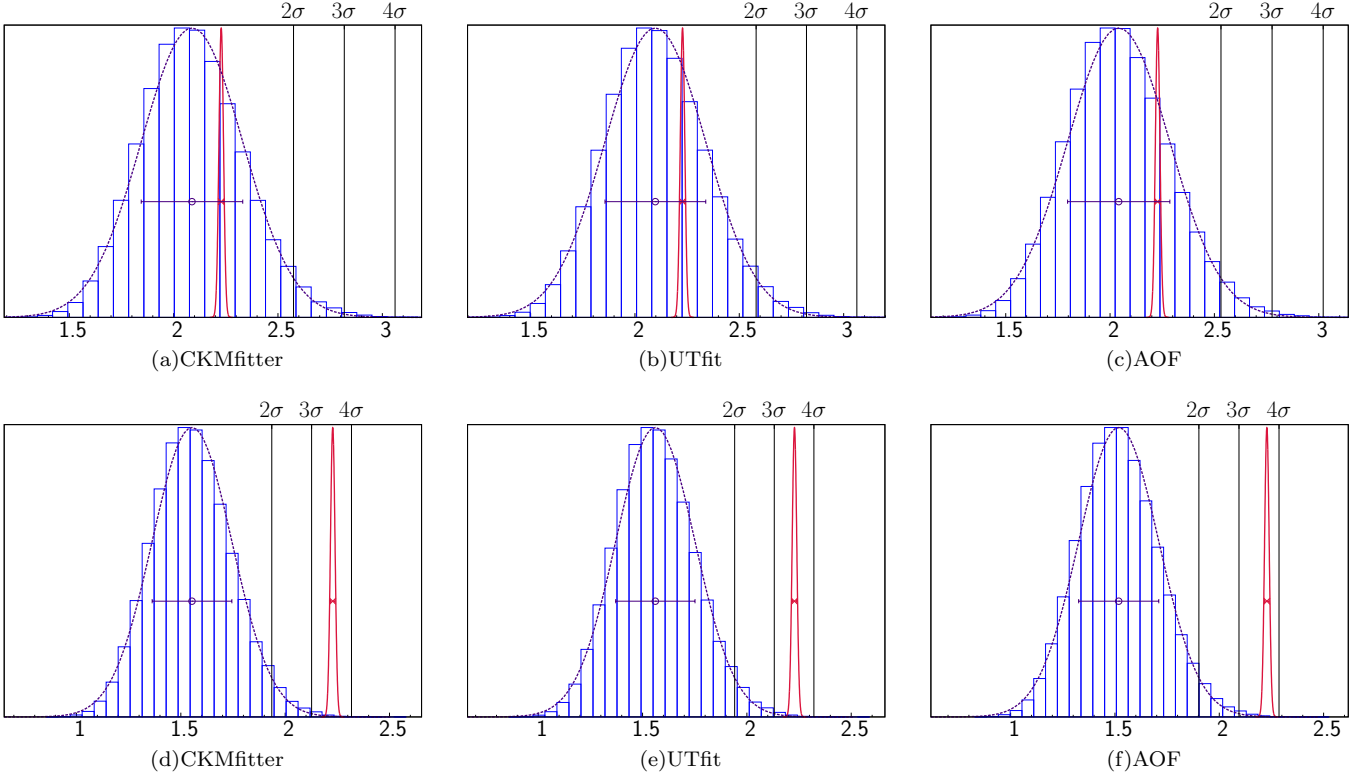


FIG. 5. Gaussian probability distributions for $\varepsilon_K^{\text{SM}}$ (blue dotted line) and $\varepsilon_K^{\text{Exp}}$ (red solid line) with the SWME \hat{B}_K . Here, we assume no correlation between \hat{B}_K and V_{cb} . Results of 5(a), 5(b) and 5(c) are obtained using the inclusive V_{cb} . Results of 5(d), 5(e) and 5(f) are obtained using the exclusive V_{cb} .

TABLE X. $\varepsilon_K^{\text{SM}}$ in units of 10^{-3} . We use the SWME \hat{B}_K with no correlation between \hat{B}_K and V_{cb} .

Input Method	Inclusive V_{cb}	Exclusive V_{cb}
CKMfitter	2.09(24)	1.55(20)
UTfit	2.10(24)	1.56(19)
AOF	2.04(25)	1.52(19)

TABLE XI. $\Delta\varepsilon_K$ with no correlation between \hat{B}_K and V_{cb} . We take $\varepsilon_K^{\text{SM}}$ from Table X. $\varepsilon_K^{\text{Exp}}$ is given in Eq. (2).

Input Method	Inclusive V_{cb}	Exclusive V_{cb}
CKMfitter	0.58σ	3.5σ
UTfit	0.54σ	3.5σ
AOF	0.76σ	3.7σ

Hence, we obtain the final results for $\Delta\varepsilon_K$ for the SWME \hat{B}_K and exclusive V_{cb} :

$$\Delta\varepsilon_K = (3.7 \pm 0.2 \pm 0.6)\sigma, \quad (\text{B1})$$

where the first error represents the ambiguity in the input methods and the second error represents the uncertainty due to the correlation between \hat{B}_K and exclusive V_{cb} .

TABLE XII. $\varepsilon_K^{\text{SM}}$ in units of 10^{-3} . We use the SWME \hat{B}_K and the exclusive V_{cb} with +50% correlation and -50% anti-correlation between them.

Input Method	$c = -50\%$	$c = +50\%$
CKMfitter	1.55(16)	1.56(22)
UTfit	1.56(16)	1.56(22)
AOF	1.52(17)	1.52(22)

TABLE XIII. $\Delta\varepsilon_K$ with +50% correlation and -50% anti-correlation between \hat{B}_K and exclusive V_{cb} . We take $\varepsilon_K^{\text{SM}}$ from Table XII. $\varepsilon_K^{\text{Exp}}$ is given in Eq. (2).

Input Method	$c = -50\%$	$c = +50\%$
CKMfitter	4.1σ	3.1σ
UTfit	4.1σ	3.1σ
AOF	4.3σ	3.3σ

First, the results in Eq. (B1) are consistent with those in Eq. (87) within the systematic errors. Second, the correlation between \hat{B}_K and exclusive V_{cb} dominates the error in $\Delta\varepsilon_K$ with the SWME \hat{B}_K . In addition, this error is much larger than that in our final results in Eq. (87).

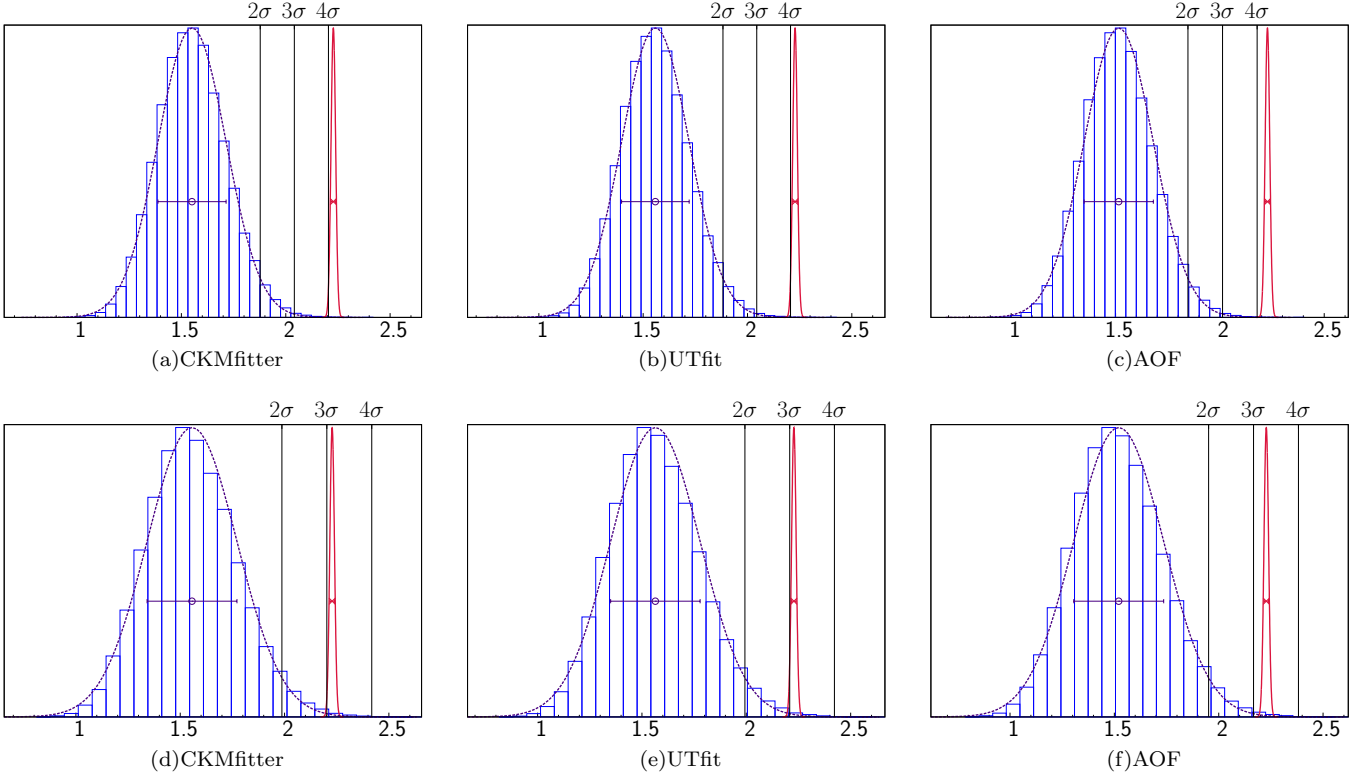


FIG. 6. Gaussian probability distributions for $\varepsilon_K^{\text{SM}}$ and $\varepsilon_K^{\text{Exp}}$ with the SWME \hat{B}_K and exclusive V_{cb} . Results of 6(a), 6(b), and 6(c) are obtained with -50% anti-correlation between \hat{B}_K and V_{cb} . Those of 6(d), 6(e), and 6(f) are obtained with $+50\%$ correlation between \hat{B}_K and V_{cb} .

Hence, we use the results with the SWME \hat{B}_K only to cross-check those with the FLAG \hat{B}_K .

-
- [1] J. Christenson, J. Cronin, V. Fitch, and R. Turlay, Phys.Rev.Lett. **13**, 138 (1964).
[2] A. Alavi-Harati et al. (KTeV Collaboration), Phys.Rev.Lett. **83**, 22 (1999), hep-ex/9905060.
[3] V. Fanti et al. (NA48 Collaboration), Phys.Lett. **B465**, 335 (1999), hep-ex/9909022.
[4] J. Beringer et al. (Particle Data Group), Phys.Rev. **D86**, 010001 (2012).
[5] M. Kobayashi and T. Maskawa, Prog.Theor.Phys. **49**, 652 (1973).
[6] N. Cabibbo, Phys.Rev.Lett. **10**, 531 (1963).
[7] N. Christ, T. Izubuchi, C. Sachrajda, A. Soni, and J. Yu (RBC and UKQCD Collaborations), Phys.Rev. **D88**, 014508 (2013), 1212.5931.
[8] N. Christ, T. Izubuchi, C. T. Sachrajda, A. Soni, and J. Yu (RBC and UKQCD), PoS **LATTICE2013**, 397 (2014), 1402.2577.
[9] A. J. Buras and D. Guadagnoli, Phys.Rev. **D78**, 033005 (2008), 0805.3887.
[10] S. Aoki, Y. Aoki, C. Bernard, T. Blum, G. Colangelo, et al. (2013), 1310.8555.
[11] T. Bae, Y.-C. Jang, H. Jeong, J. Kim, J. Kim, et al., PoS **LATTICE2013**, 476 (2014), 1310.7319.
[12] R. Arthur et al. (RBC Collaboration, UKQCD Collaboration), Phys.Rev. **D87**, 094514 (2013), 1208.4412.
[13] J. Laiho and R. S. Van de Water, PoS **LATTICE2011**, 293 (2011), 1112.4861.
[14] T. Bae et al., Phys.Rev.Lett. **109**, 041601 (2012), 1111.5698.
[15] S. Durr, Z. Fodor, C. Hoelbling, et al., Phys.Lett. **B705**, 477 (2011), 1106.3230.
[16] T. Bae et al. (SWME Collaboration), Phys.Rev. **D89**, 074504 (2014), 1402.0048.
[17] T. Blum, P. Boyle, N. Christ, N. Garron, E. Goode, et al., Phys.Rev.Lett. **108**, 141601 (2012), 1111.1699.
[18] J. A. Bailey, A. Bazavov, C. Bernard, et al., Phys.Rev. **D89**, 114504 (2014), 1403.0635.
[19] P. Gambino and C. Schwanda, Phys.Rev. **D89**, 014022 (2014), 1307.4551.
[20] A. Alberti, P. Gambino, K. J. Healey, and S. Nandi, Phys.Rev.Lett. **114**, 061802 (2015), 1411.6560.
[21] N. Uraltsev (2000), hep-ph/0010328.
[22] G. Buchalla, A. J. Buras, and M. E. Lautenbacher, Rev.Mod.Phys. **68**, 1125 (1996), hep-ph/9512380.
[23] J. Charles et al. (CKMfitter Group), Eur.Phys.J. **C41**, 1 (2005), hep-ph/0406184.
[24] A. Hocker, H. Lacker, S. Laplace, and F. Le Diberder, Eur.Phys.J. **C21**, 225 (2001), hep-ph/0104062.

- [25] M. Bona et al. (UTfit Collaboration), JHEP **0507**, 028 (2005), hep-ph/0501199.
- [26] M. Bona et al. (UTfit Collaboration), JHEP **0803**, 049 (2008), 0707.0636.
- [27] A. Bevan, M. Bona, M. Ciuchini, D. Derkach, E. Franco, et al., Nucl.Phys.Proc.Suppl. **241-242**, 89 (2013).
- [28] A. J. Buras, pp. 281–539 (1998), to appear in 'Probing the Standard Model of Particle Interactions', F.David and R. Gupta, eds., 1998, Elsevier Science B.V., hep-ph/9806471.
- [29] V. Weisskopf and E. P. Wigner, Z.Phys. **63**, 54 (1930).
- [30] V. Weisskopf and E. Wigner, Z.Phys. **65**, 18 (1930).
- [31] Q. Wang and A. Sanda, Phys.Rev. **D55**, 3131 (1997).
- [32] B. Winstein and L. Wolfenstein, Rev.Mod.Phys. **65**, 1113 (1993).
- [33] S. Pokorski, *Gauge Field Theories 2nd Ed.* (Cambridge University Press, 2000).
- [34] Y.-B. Liang and Q. Wang, J.Phys. **G27**, 243 (2001).
- [35] V. Cirigliano, G. Ecker, H. Neufeld, A. Pich, and J. Portoles, Rev.Mod.Phys. **84**, 399 (2012), 1107.6001.
- [36] G. Branco, L. Lavoura, and J. Silva, *CP Violation*, International series of monographs on physics (Clarendon Press, 1999), ISBN 9780198503996.
- [37] J. Donoghue, E. Golowich, and B. R. Holstein, *Dynamics of the standard model* (Camb.Monogr.Part.Phys.Nucl.Phys.Cosmol., 1992).
- [38] A. J. Buras, D. Guadagnoli, and G. Isidori, Phys.Lett. **B688**, 309 (2010), 1002.3612.
- [39] T. Inami and C. Lim, Prog.Theor.Phys. **65**, 297 (1981).
- [40] K. Chetyrkin, J. H. Kuhn, and M. Steinhauser, Comput.Phys.Commun. **133**, 43 (2000), hep-ph/0004189.
- [41] S. Herrlich and U. Nierste, Nucl.Phys. **B476**, 27 (1996), hep-ph/9604330.
- [42] Z. Bai, N. Christ, T. Izubuchi, C. Sachrajda, A. Soni, et al., Phys.Rev.Lett. **113**, 112003 (2014), 1406.0916.
- [43] A. X. El-Khadra, A. S. Kronfeld, and P. B. Mackenzie, Phys. Rev. **D55**, 3933 (1997), hep-lat/9604004.
- [44] J. Harada, S. Hashimoto, A. S. Kronfeld, and T. Onogi, Phys.Rev. **D65**, 094514 (2002), hep-lat/0112045.
- [45] J. Harada, S. Hashimoto, K.-I. Ishikawa, A. S. Kronfeld, T. Onogi, et al., Phys.Rev. **D65**, 094513 (2002), hep-lat/0112044.
- [46] A. S. Kronfeld, Phys.Rev. **D62**, 014505 (2000), hep-lat/0002008.
- [47] A. Bazavov, D. Toussaint, C. Bernard, J. Laiho, C. DeTar, et al., Rev.Mod.Phys. **82**, 1349 (2010), 0903.3598.
- [48] Y. Amhis et al. (Heavy Flavor Averaging Group) (2012), 1207.1158.
- [49] Y. Aoki, R. Arthur, T. Blum, et al., Phys.Rev. **D84**, 014503 (2011), 1012.4178.
- [50] C. Aubin, J. Laiho, and R. S. Van de Water, Phys.Rev. **D81**, 014507 (2010), 0905.3947.
- [51] J. Brod and M. Gorbahn, Phys.Rev. **D82**, 094026 (2010), 1007.0684.
- [52] J. Brod and M. Gorbahn, Phys.Rev.Lett. **108**, 121801 (2012), 1108.2036.
- [53] J. A. Bailey, Y.-C. Jang, and W. Lee (SWME Collaboration), PoS **LATTICE2014**, 371 (2014), 1410.6995.
- [54] A. J. Buras and J. Gorbach, Eur.Phys.J. **C73**, 2560 (2013), 1304.6835.
- [55] S. Alekhin, A. Djouadi, and S. Moch, Phys.Lett. **B716**, 214 (2012), 1207.0980.
- [56] <http://www.gnu.org/software/gsl/>.
- [57] M. Luscher, Comput.Phys.Commun. **79**, 100 (1994), hep-lat/9309020.
- [58] J. Laiho, E. Lunghi, and R. S. Van de Water, Phys.Rev. **D81**, 034503 (2010), <http://latticeaverages.org/>, 0910.2928.
- [59] Y.-C. Jang and W. Lee, PoS **LATTICE2012**, 269 (2012), 1211.0792.
- [60] A. J. Buras, F. De Fazio, and J. Gorbach, Eur.Phys.J. **C74**, 2950 (2014), 1404.3824.
- [61] A. J. Buras and J. Gorbach, Rept.Prog.Phys. **77**, 086201 (2014), 1306.3775.
- [62] M. B. Oktay and A. S. Kronfeld, Phys.Rev. **D78**, 014504 (2008), 0803.0523.
- [63] Y.-C. Jang et al. (SWME, MILC, Fermilab Lattice), PoS **LATTICE2013**, 030 (2014), 1311.5029.
- [64] J. A. Bailey, Y.-C. Jang, W. Lee, and J. Leem (SWME Collaboration), PoS **LATTICE2014**, 389 (2014), 1411.4227.
- [65] J. A. Bailey, Y.-C. Jang, W. Lee, C. DeTar, A. S. Kronfeld, et al., PoS **LATTICE2014**, 097 (2014), 1411.1823.
- [66] K. Chetyrkin, B. A. Kniehl, and M. Steinhauser, Phys.Rev.Lett. **79**, 2184 (1997), hep-ph/9706430.
- [67] S. Herrlich and U. Nierste, Nucl.Phys. **B419**, 292 (1994), hep-ph/9310311.
- [68] M. Steinhauser, Comput.Phys.Commun. **134**, 335 (2001), hep-ph/0009029.
- [69] M. Gorbahn and U. Haisch, Nucl.Phys. **B713**, 291 (2005), hep-ph/0411071.
- [70] A. J. Buras, M. Gorbahn, U. Haisch, and U. Nierste, JHEP **11**, 002 (2006), hep-ph/0603079.